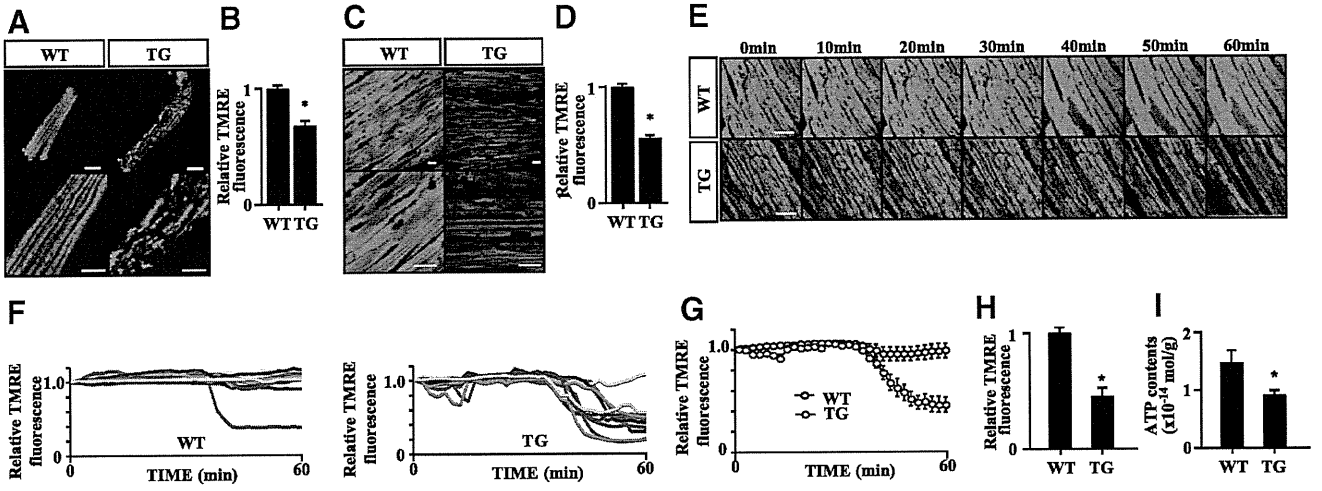

Figure 5. Reduced TMRE fluorescence in cardiomyocytes from p300ΔC/H3-TG hearts. A, Images of isolated TMRE-stained ventricular myocytes from WT and p300ΔC/H3-TG hearts. Scale bars=20 μm (top) or 10 μm (bottom). B, TMRE fluorescence of each mitochondrion in TMRE loaded isolated cardiac myocyte. The average of relative TMRE fluorescence of mitochondrion in WT cardiac myocytes was assigned a value of 1.0. C, Imaging of mitochondria in WT and p300ΔC/H3-TG hearts perfused with Tyrode's solution containing TMRE using the Langendorff method. Scale bar=20 μm. D, TMRE fluorescence of each mitochondrion of TMRE perfused in ex vivo mouse hearts. The average of relative TMRE fluorescence of mitochondrion in WT hearts was assigned a value of 1.0. E, Representative images showing progressive loss of mitochondrial membrane potential during ischemia. Images were acquired every 10 minutes. Images are from a single experiment representative of at least 3 independent experiments. Scale bar=50 μm. F, Time course of relative TMRE fluorescence intensities in several individual cells monitored at 2-minute intervals. TMRE fluorescence intensity at 0 minutes in each cell was assigned a value of 1.0. G, Average of relative TMRE fluorescence intensities in individual cells of WT and p300ΔC/H3-TG hearts monitored at 2-minute intervals. TMRE fluorescence intensity at 0 minutes in each cell was assigned a value of 1.0. H, TMRE fluorescence from individual cells in WT and p300ΔC/H3-TG hearts subjected to ischemia for 60 minutes. The relative TMRE fluorescence in WT hearts subjected to ischemia for 60 minutes was assigned a value of 1.0. I, ATP contents in WT and p300ΔC/H3-TG hearts. In all graphs, bars represent means±SEM.

It is known that PGC-1α, ERRα and PPARα act in concert to regulate mitochondrial biogenesis through the regulation of mitochondrial gene expression.[14,15,17] PGC-1α regulates the expression and transcriptional activity of ERRα,[37] whereas PGC-1α and ERRα act synergistically to activate the PPARα promoter.[13] Although p300 reportedly interacts with both PGC-1α and PPARα, its role in the transcriptional control of mitochondrial gene expression is not fully understood.[18–20] In the present study, we found that p300 is an indispensable component of the transcriptional pathways via which mitochondrial gene expression is regulated in adult ventricles. Indeed, transcription of ERRα, PPARα, and PGC-1α was significantly downregulated in p300ΔC/H3-TG hearts, which would in turn disrupt expression of an array of mitochondrial genes, leading to severe structural and functional abnormalities in mitochondria from p300ΔC/H3-TG mice.

p300 also serves as a cofactor for the cardiac-enriched transcription factors GATA4 and MEF2, which participate in the transcriptional regulation of fetal cardiac genes such as ANP and BNP.[7,38] Here, we confirmed that p300ΔC/H3 significantly inhibits GATA4- and MEF2-dependent promoter activity in cultured cells and showed that the activities of the ANP and BNP promoters were diminished by p300ΔC/H3 in cultured neonatal rat ventricular myocytes and noncardiomyocytes. Unexpectedly, however, expression of ANP and BNP mRNA was strongly upregulated in p300ΔC/H3-TG hearts (Figure 3A). Although it is clear that p300 coactivates GATA4 and MEF2C, our data suggest that p300 is dispensable for the pathological induction of ANP and BNP expression in the adult heart.

Mitochondria play a crucial role in the regulation of cell survival. Their dysfunction can lead to apoptosis, autophagy, and other modes of cell death via various pathways involving caspase activation, endoplasmic/sarcoplasmic reticulum–mitochondria connections and lysosome-mitochondria crosstalk.[35] In the present study, we found that the abnormal mitochondrial gene expression and function seen in p300ΔC/H3-TG hearts led to myocardial cell death that, at least in part, was caused by autophagy; we found no evidence of apoptotic cell death. Consistent with those results are the recent findings that mitochondrial apoptotic pathways are defective in cardiac myocytes.[39–41] For instance, the expression of apoptotic peptidase activating factor-1, an essential mediator of mitochondrial apoptotic death pathways, is suppressed in cardiac myocytes, making them resistant to mitochondria-mediated apoptosis.[41]

In summary, we found that, through the regulation of transcriptional pathways controlling mitochondrial gene expression, p300 is critically involved in the maintenance of mitochondrial integrity and cell survival in adult ventricles. These findings provide novel insight that could be useful in the development of new therapeutic strategies aimed at

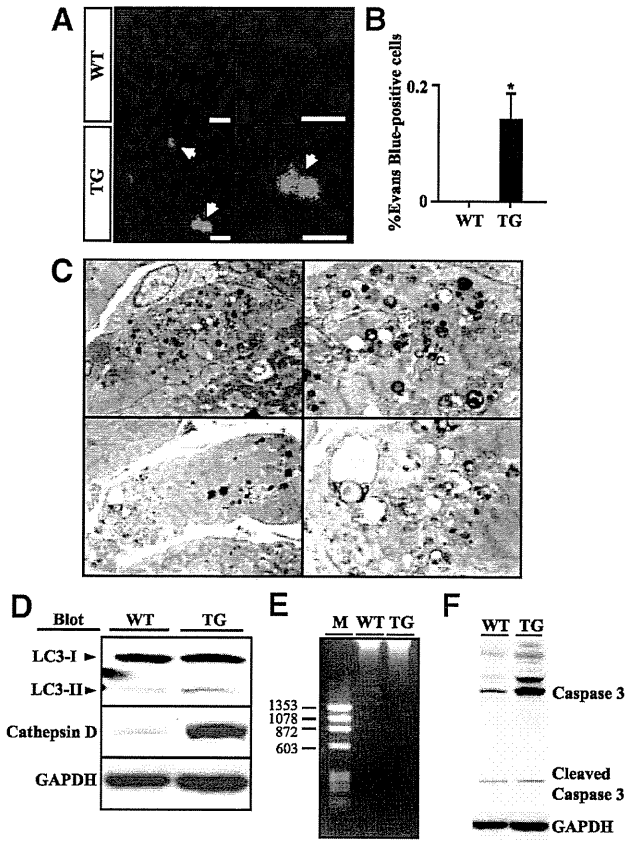

Figure 6. Analysis of cell death in p300ΔC/H3-TG hearts. A, Myocardia of a WT and a p300ΔC/H3-TG mouse intraperitoneally injected with Evans blue dye are shown. Red fluorescence indicates uptake of Evans blue (cell death). The nuclei appear blue. Scale bars=10 μm. B, Graphs show the numbers of Evans blue positive cells in WT and p300ΔC/H3-TG hearts. Bars represent means±SEM. C, Transmission electron micrographs of cardiac myocytes from a 12-weeks-old p300ΔC/H3-TG mouse showing the presence of autophagosomes. Left images show lower magnification; right images, higher magnification. D, Western blot analysis of LC-3 and cathepsin D in hearts from 12-week-old WT and p300ΔC/H3-TG mice. E, Ladder analysis of genomic DNA from 12-week-old WT and p300ΔC/H3-TG mice. F, Western blot analysis of full-length and cleaved caspase-3 in cardiac tissue from 12-week-old WT and p300ΔC/H3-TG mice.

preserving cardiac mitochondrial function through the enhancement of p300 activity.

Acknowledgments

We thank Y. Kubo for excellent secretarial work. We also thank N. Mizushima for providing the anti-LC3 antibody.

Sources of Funding

This research was supported by a Grant-in-Aid for Scientific Research from the Japan Society for the Promotion of Science (to K.K., M.H., and K.N.) and grants from the Japanese Ministry of Health, Labor and Welfare (to K.N.); the Japan Heart Foundation/Pfizer Pharmaceuticals Inc Grant on Cardiovascular Disease Research; the Japan Heart Foundation/Novartis Grant for Research Award on Molecular and Cellular Cardiology; the Mochida Memorial Foundation for Medical and Pharmaceutical Research; the Uehara Memorial Foundation; the Ichiro Kanehara Foundation; the Astellas Foundation for Research on Metabolic Disorders; the Mitsubishi Foundation; the Suzuken Memorial Foundation; the Takeda Medical Research Foundation; and the Kanae Foundation for the Promotion of Medical Science (to K.K.).

Disclosures

None.

References

1. Ogryzko VV, Schiltz RL, Russanova V, Howard BH, Nakatani Y. The transcriptional coactivators p300 and CBP are histone acetyltransferases. *Cell.* 1996;87:953–959.
2. Eckner R, Ewen ME, Newsome D, Gerdes M, DeCaprio JA, Lawrence JB, Livingston DM. Molecular cloning and functional analysis of the adenovirus E1A-associated 300-kD protein (p300) reveals a protein with properties of a transcriptional adaptor. *Genes Dev.* 1994;8:869–884.
3. Yao TP, Oh SP, Fuchs M, Zhou ND, Ch'ng LE, Newsome D, Bronson RT, Li E, Livingston DM, Eckner R. Gene dosage-dependent embryonic development and proliferation defects in mice lacking the transcriptional integrator p300. *Cell.* 1998;93:361–372.
4. Dai YS, Markham BE. p300 Functions as a coactivator of transcription factor GATA-4. *J Biol Chem.* 2001;276:37178–37185.
5. Slepak TI, Webster KA, Zang J, Prentice H, O'Dowd A, Hicks MN, Bishopric NH. Control of cardiac-specific transcription by p300 through myocyte enhancer factor-2D. *J Biol Chem.* 2001;276:7575–7585.
6. Kakita T, Hasegawa K, Morimoto T, Kaburagi S, Wada H, Sasayama S. p300 protein as a coactivator of GATA-5 in the transcription of cardiac-restricted atrial natriuretic factor gene. *J Biol Chem.* 1999;274:34096–34102.
7. Yanazume T, Hasegawa K, Morimoto T, Kawamura T, Wada H, Matsumori A, Kawase Y, Hirai M, Kita T. Cardiac p300 is involved in myocyte growth with decompensated herat failure. *Mol Cell Biol.* 2003;23:3593–3606.
8. Miyamoto S, Kawamura T, Morimoto T, Ono K, Wada H, Kawase Y, Matsumori A, Nishio R, Kita T, Hasegawa K. Histone acetyltransferase activity of p300 is required for the promotion of left ventricular remodeling after myocardial infarction in adult mice in vivo. *Circulation.* 2006;113:679–690.
9. Morimoto T, Sunagawa Y, Kawamura T, Takaya T, Wada H, Nagasawa A, Komeda M, Fujita M, Shimatsu A, Kita T, Hasegawa K. The dietary compound curcumin inhibits p300 histone acetyltransferase activity and prevents heart failure in rats. *J Clin Invest.* 2008;118:868–878.
10. Shikama N, Lutz W, Kretzschmar R, Sauter N, Roth JF, Marino S, Wittwer J, Scheidweiler A, Eckner R. Essential function of p300 acetyltransferase activity in heart, lung and small intestine formation. *EMBO J.* 2003;22:5175–5185.
11. Kawamura T, Hasegawa K, Morimoto T, Iwai-Kanai E, Miyamoto S, Kawase Y, Ono K, Wada H, Akao M, Kita T. Expression of p300 protects cardiac myocytes from apoptosis in vivo. *Biochem Biophys Res Commun.* 2004;315:733–738.
12. Lehman JJ, Barger PM, Kovacs A, Saffitz JE, Medeiros DM, Kelly DP. Peroxisome proliferator-activated receptor gamma coactivator-1 promotes cardiac mitochondrial biogenesis. *J Clin Invest.* 2000;106:847–856.
13. Huss JM, Torra IP, Staels B, Giguere V, Kelly DP. Estrogen-related receptor alpha directs peroxisome proliferator-activated receptor alpha signaling in the transcriptional control of energy metabolism in cardiac and skeletal muscle. *Mol Cell Biol.* 2004;24:9079–9091.
14. Gulick T, Cresci S, Caira T, Moore DD, Kelly DP. The peroxisome proliferator-activated receptor regulates mitochondrial fatty acid oxidative enzyme gene expression. *Proc Natl Acad Sci U S A.* 1994;91:11012–11016.
15. Finck BN, Kelly DP. Peroxisome proliferator-activated receptor gamma coactivator-1 (PGC-1) regulatory cascade in cardiac physiology and disease. *Circulation.* 2007;115:2540–2548.
16. Puigserver P, Wu Z, Park CW, Graves R, Wright M, Spiegelman BM. A cold-inducible coactivator of nuclear receptors linked to adaptive thermogenesis. *Cell.* 1998;92:829–839.
17. Schreiber SN, Emter R, Hock MB, Knutti D, Cardenas J, Podvinec M, Oakeley EJ, Kralli A. The estrogen-related receptor alpha (ERRalpha) functions in PPARgamma coactivator 1alpha (PGC-1alpha)-induced mitochondrial biogenesis. *Proc Natl Acad Sci U S A.* 2004;101:6472–6477.
18. Puigserver P, Adelmant G, Wu Z, Fan M, Xu J, O'Malley B, Spiegelman BM. Activation of PPARgamma coactivator-1 through transcription factor docking. *Science.* 1999;286:1368–1371.

19. Wallberg AE, Yamamura S, Malik S, Spiegelman B, Roeder RG. Coordination of p300-mediated chromatin remodeling and TRAP/mediator function through coactivator PGC-1a. *Mol Cell.* 2003;12:1137–1149.
20. Dowell P, Ishmael JE, Avram D, Peterson VJ, Nevrivy DJ, Leid M. p300 functions as a coactivator for the peroxisome proliferator-activated receptor alpha. *J Biol Chem.* 1997;272:33435–33443.
21. Kuwahara K, Saito Y, Ogawa E, Takahashi N, Nakagawa Y, Naruse Y, Harada M, Hamanaka I, Izumi T, Miyamoto Y, Kishimoto I, Kawakami R, Nakanishi M, Mori N, Nakao K. The neuron-restrictive silencer element-neuron-restrictive silencer factor system regulates basal and endothelin 1-inducible atrial natriuretic peptide gene expression in ventricular myocytes. *Mol Cell Biol.* 2001;21:2085–2097.
22. Ogawa E, Saito Y, Kuwahara K, Harada M, Miyamoto Y, Hamanaka I, Kajiyama N, Takahashi N, Izumi T, Kawakami R, Kishimoto I, Naruse Y, Mori N, Nakao K. Fibronectin signaling stimulates BNP gene transcription by inhibiting neuron-restrictive silencer element-dependent repression. *Cardiovasc Res.* 2002;53:451–459.
23. Nakagawa O, Ogawa Y, Itoh H, Suga S, Komatsu Y, Kishimoto I, Nishino K, Yoshimasa T, Nakao K. Rapid transcriptional activation and early mRNA turnover of brain natriuretic peptide in cardiocyte hypertrophy. Evidence for brain natriuretic peptide as an "emergency" cardiac hormone against ventricular overload. *J Clin Invest.* 1995;96:1280–1287.
24. Kuwahara K, Saito Y, Takano M, Arai Y, Yasuno S, Nakagawa Y, Takahashi N, Adachi Y, Takemura G, Horie M, Miyamoto Y, Morisaki T, Kuratomi S, Noma A, Fujiwara H, Yoshimasa Y, Kinoshita H, Kawakami R, Kishimoto I, Nakanishi M, Usami S, Saito Y, Harada M, Nakao K. NRSF regulates the fetal cardiac gene program and maintains normal cardiac structure and function. *EMBO J.* 2003;22:6310–6321.
25. Kabeya Y, Mizushima N, Ueno T, Yamamoto A, Kirisako T, Noda T, Kominami E, Ohsumi Y, Yoshimori T. LC3, a mammalian homologue of yeast Apg8p, is localized in autophagosome membranes after processing. *EMBO J.* 2000;19:5720–5728.
26. Kuma A, Hatano M, Matsui M, Yamamoto A, Nakaya H, Yoshimori T, Ohsumi Y, Tokuhisa T, Mizushima N. The role of autophagy during the early neonatal starvation period. *Nature.* 2004;432:1032–1036.
27. Matsumoto-Ida M, Akao M, Takeda T, Kato M, Kita T. Real-time 2-photon imaging of mitochondrial function in perfused rat hearts subjected to ischemia/reperfusion. *Circulation.* 2006;114:1497–1503.
28. De Luca A, Severino A, De Paolis P, Cottone G, De Luca L, De Falco M, Porcellini A, Volpe M, Condorelli G. p300/cAMP-response-element-binding-protein ('CREB')-binding protein (CBP) modulates co-operation between myocyte enhancer factor 2A (MEF2A) and thyroid hormone receptor-retinoid X receptor. *Biochem J.* 2003;369:477–484.
29. Avantaggiati ML, Ogryzko V, Gardner K, Giordano A, Levine AS, Kelly K. Recruitment of p300/CBP in p53-dependent signal pathways. *Cell.* 1997;89:1175–1184.
30. Yang XJ, Ogryzko VV, Nishikawa J, Howard BH, Nakatani Y. A p300/CBP-associated factor that competes with the adenoviral oncoprotein E1A. *Nature.* 1996;382:319–324.
31. Saito Y, Nakao K, Arai H, Nishimura K, Okumura K, Obata K, Takemura G, Fujiwara H, Sugawara A, Yamada T. Augmented expression of atrial natriuretic polypeptide gene in ventricle of human failing heart. *J Clin Invest.* 1989;83:298–305.
32. Mukoyama M, Nakao K, Hosoda K, Suga S, Saito Y, Ogawa Y, Shirakami G, Jougasaki M, Obata K, Yasue H. Brain natriuretic peptide as a novel cardiac hormone in humans. Evidence for an exquisite dual natriuretic peptide system, atrial natriuretic peptide and brain natriuretic peptide. *J Clin Invest.* 1991;87:1402–1412.
33. Czubryt MP, McAnally J, Fishman GI, Olson EN. Regulation of peroxisome proliferator-activated receptor gamma coactivator 1 alpha (PGC-1 alpha) and mitochondrial function by MEF2 and HDAC5. *Proc Natl Acad Sci U S A.* 2003;100:1711–1716.
34. Wei JQ, Shehadeh LA, Mitrani JM, Pessanha M, Slepak TI, Webster KA, Bishopric NH. Quantitative control of adaptive cardiac hypertrophy by acetyltransferase p300. *Circulation.* 2008;118:934–946.
35. Kim R, Emi M, Tanabe K. Role of mitochondria as the gardens of cell death. *Cancer Chemother Pharmacol.* 2006;57:545–553.
36. Miyata S, Takemura G, Kawase Y, Li Y, Okada H, Maruyama R, Ushikoshi H, Esaki M, Kanamori H, Li L, Misao Y, Tezuka A, Toyo-Oka T, Minatoguchi S, Fujiwara T, Fujiwara H. Autophagic cardiomyocyte death in cardiomyopathic hamsters and its prevention by granulocyte colony-stimulating factor. *Am J Pathol.* 2006;168:386–397.
37. Schreiber SN, Knutti D, Brogli K, Uhlmann T, Kralli A. The transcriptional coactivator PGC-1 regulates the expression and activity of the orphan nuclear receptor estrogen-related receptor alpha (ERRalpha). *J Biol Chem.* 2003;278:9013–9018.
38. Gusterson R, Brar B, Faulkes D, Giordano A, Chrivia J, Latchman D. The transcriptional co-activators CBP and p300 are activated via phenylephrine through the p42/p44 MAPK cascade. *J Biol Chem.* 2002;277:2517–2524.
39. Kanoh M, Takemura G, Misao J, Hayakawa Y, Aoyama T, Nishigaki K, Noda T, Fujiwara T, Fukuda K, Minatoguchi S, Fujiwara H. Significance of myocytes with positive DNA in situ nick end-labeling (TUNEL) in hearts with dilated cardiomyopathy: not apoptosis but DNA repair. *Circulation.* 1999;99:2757–2764.
40. Takemura G, Fujiwara H. Morphological aspects of apoptosis in heart diseases. *J Cell Mol Med.* 2006;10:56–75.
41. Bahi N, Zhang J, Llovera M, Ballester M, Comella JX, Sanchis D. Switch from caspase-dependent to caspase-independent death during heart development: essential role of endonuclease G in ischemia-induced DNA processing of differentiated cardiomyocytes. *J Biol Chem.* 2006;281:22943–22952.

T-Type Ca^{2+} Channel Blockade Prevents Sudden Death in Mice With Heart Failure

Hideyuki Kinoshita, MD; Koichiro Kuwahara, MD, PhD; Makoto Takano, MD, PhD; Yuji Arai, MD, PhD; Yoshihiro Kuwabara, MD; Shinji Yasuno, MD; Yasuaki Nakagawa, MD, PhD; Michio Nakanishi, MD, PhD; Masaki Harada, MD, PhD; Masataka Fujiwara, MD; Masao Murakami, PhD; Kenji Ueshima, MD, PhD; Kazuwa Nakao, MD, PhD

Background—Pharmacological interventions for prevention of sudden arrhythmic death in patients with chronic heart failure remain limited. Accumulating evidence suggests increased ventricular expression of T-type Ca^{2+} channels contributes to the progression of heart failure. The ability of T-type Ca^{2+} channel blockade to prevent lethal arrhythmias associated with heart failure has never been tested, however.

Methods and Results—We compared the effects of efonidipine and mibefradil, dual T- and L-type Ca^{2+} channel blockers, with those of nitrendipine, a selective L-type Ca^{2+} channel blocker, on survival and arrhythmogenicity in a cardiac-specific, dominant-negative form of neuron-restrictive silencer factor transgenic mice (dnNRSF-Tg), which is a useful mouse model of dilated cardiomyopathy leading to sudden death. Efonidipine, but not nitrendipine, substantially improved survival among dnNRSF-Tg mice. Arrhythmogenicity was dramatically reduced in dnNRSF-Tg mice treated with efonidipine or mibefradil. Efonidipine acted by reversing depolarization of the resting membrane potential otherwise seen in ventricular myocytes from dnNRSF-Tg mice and by correcting cardiac autonomic nervous system imbalance. Moreover, the *R*(−)-isomer of efonidipine, a recently identified, highly selective T-type Ca^{2+} channel blocker, similarly improved survival among dnNRSF-Tg mice. Efonidipine also reduced the incidence of sudden death and arrhythmogenicity in mice with acute myocardial infarction.

Conclusions—T-type Ca^{2+} channel blockade reduced arrhythmias in a mouse model of dilated cardiomyopathy by repolarizing the resting membrane potential and improving cardiac autonomic nervous system imbalance. T-type Ca^{2+} channel blockade also prevented sudden death in mice with myocardial infarction. Our findings suggest T-type Ca^{2+} channel blockade is a potentially useful approach to preventing sudden death in patients with heart failure. (***Circulation.* 2009;120:743-752.**)

Key Words: ion channels ■ nervous system, autonomic ■ heart failure ■ calcium ■ arrhythmia

As many as 50% of deaths among heart failure patients are sudden and unexpected, presumably the result of lethal arrhythmias.[1] Despite recent progress in nonpharmacological therapy, pharmacological interventions for the treatment and prevention of lethal arrhythmias associated with chronic heart failure remain limited. A prerequisite for the development of new pharmacological approaches is to identify potential targets based on knowledge of the molecular basis of arrhythmogenesis in failing hearts.

Clinical Perspective on p 752

Compelling evidence implicates T-type Ca^{2+} channels in the progression of heart failure.[2,3] During development, T-type Ca^{2+} channels are abundantly expressed in the embryonic ventricle, but their expression is suppressed in the adult ventricle, so that it is restricted to the conduction system.[4,5] However, T-type Ca^{2+} channels are reexpressed in hypertrophied and failing ventricles,[4,6–9] and the resultant T-type Ca^{2+} currents ($I_{Ca,T}$) are thought to be involved in the pathological process that leads to systolic dysfunction and arrhythmogenesis.[2,9] Indeed, several studies have shown that mibefradil, which blocks both T- and L-type Ca^{2+} channels, mitigates the functional deterioration of the ventricle in some animal models of heart failure.[10–12] More recently, it was shown that the genetic deletion of *CACNA1H*, which encodes the α1H T-type Ca^{2+} channel, resulted in resistance to pathological

Received February 12, 2009; accepted June 23, 2009.

From the Department of Medicine and Clinical Science (H.K., K.K., Y.K., S.Y., Y.N., M.N., M.H., M.F., M.M., K.N.), Kyoto University Graduated School of Medicine, Kyoto, Japan; Department of Biophysics (M.T.), Jichi Medical School, Shimotsuke, Japan; Department of Bioscience (Y.A.), National Cardiovascular Center Research Institute, Suita, Japan; and EBM Research Center (K.U.), Kyoto University Graduate School of Medicine, Kyoto, Japan.

The online-only Data Supplement is available with this article at http://circ.ahajournals.org/cgi/content/full/CIRCULATIONAHA.109.857011/DC1.

Correspondence to Koichiro Kuwahara, MD, PhD, Department of Medicine and Clinical Science, Kyoto University Graduated School of Medicine, 54 Shogoin Kawaracho, Sakyo-ku, Kyoto, Japan 606-8507. E-mail kuwa@kuhp.kyoto-u.ac.jp

Circulation **is available at http://circ.ahajournals.org** **DOI: 10.1161/CIRCULATIONAHA.109.857011**

cardiac hypertrophy.[9] The ability of T-type Ca^{2+} channel blockade to prevent malignant arrhythmia and sudden death associated with heart failure remains unevaluated, however.

We recently reported that a transcriptional repressor, neuron-restrictive silencer factor (NRSF, also called REST), is an important regulator of the fetal cardiac gene program.[13] Transgenic mice that selectively express a dominant-negative form of NRSF (dnNRSF) in their hearts (dnNRSF-Tg) showed progressive cardiomyopathy and sudden arrhythmic death beginning at ≈8 weeks of age.[14] The dnNRSF-Tg hearts showed increased expression of fetal-type ion channel genes, including *CACNA1H*, which encodes the T-type Ca^{2+} channel α-subunit. Moreover, $I_{Ca,T}$ amplitude was correspondingly increased in ventricular myocytes from dnNRSF-Tg hearts, which suggests that $I_{Ca,T}$ in some way contributes to the susceptibility of dnNRSF-Tg hearts to arrhythmias.[14]

To clarify the contribution made by T-type Ca^{2+} channels to the development of malignant arrhythmias and to assess the ability of T-type Ca^{2+} channel blockade to prevent sudden death associated with heart failure, we compared the effects of efonidipine and mibefradil, dual T- and L-type Ca^{2+} channel blockers,[15,16] with those of nitrendipine, a more L-type–selective Ca^{2+} channel blocker, on survival and arrhythmogenicity in dnNRSF-Tg mice and mice with myocardial infarction. We also tested the effects of the *R*(−)-isomer of efonidipine [*R*(−)-efonidipine], a recently identified, highly selective T-type Ca^{2+} channel blocker, on dnNRSF-Tg mice.[17,18] Our findings demonstrate that T-type Ca^{2+} channel blockade may represent a new and effective means of preventing sudden cardiac death in patients with heart failure.

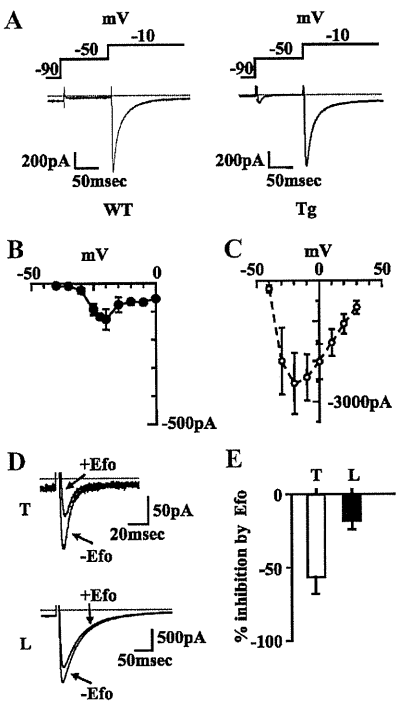

Figure 1. $I_{Ca,T}$ in ventricular myocytes from dnNRSF-Tg mice. A, Ca^{2+} currents recorded in WT (left) and dnNRSF-Tg (Tg; right) mouse. The double-pulse protocol is shown at the top. Na^+ currents were suppressed by use of Na^+-free bathing solution. $I_{Ca,T}$ were elicited at −50 mV only in dnNRSF mice. B, Current-voltage relationship for $I_{Ca,T}$ in cardiomyocytes from dnNRSF mice (n=5). At membrane potentials more positive than −40 mV, peak amplitudes of inward currents elicited from a conditioning potential of −90 or −50 mV were subtracted. C, Current-voltage relationship for $I_{Ca,L}$ in cardiomyocytes from dnNRSF mice. The conditioning potential was −50 mV (n=5). D, Effect of efonidipine (Efo) 10 μmol/L on $I_{Ca,T}$ (T) and $I_{Ca,L}$ (L). In the top panel, $I_{Ca,T}$ was activated by depolarization to −45 mV from a holding potential of −80 mV. Bottom panel, $I_{Ca,L}$ recorded from a myocyte from a WT mouse. $I_{Ca,L}$ was activated by depolarization to −10 mV from a holding potential of −80 mV. E, Summary of the inhibitory effects of efonidipine (Efo; 10 μmol/L) on $I_{Ca,T}$ (T) and $I_{Ca,L}$ (L) in ventricular myocytes. Efonidipine reduced the amplitudes of $I_{Ca,T}$ by 57±12% (n=4) while reducing the amplitudes of $I_{Ca,L}$ by 21±4% (n=5).

Methods

Animal Experiments

Animal care and all experimental protocols were conducted in accordance with the institutional guidelines of the Kyoto University Graduate School of Medicine. Beginning at 8 weeks of age, dnNRSF-Tg mice were left untreated (control) or were treated for 7 weeks with efonidipine (40 mg · kg^{-1} · d^{-1} PO) or nitrendipine (20 mg · kg^{-1} · d^{-1} PO). In another experiment, 10- or 11-week-old dnNRSF-Tg mice were left untreated (control) or treated for 7 days with mibefradil (15 mg · kg^{-1} · d^{-1}), efonidipine (200 mg · kg^{-1} · d^{-1}), or nitrendipine (60 mg · kg^{-1} · d^{-1}). The doses of mibefradil, efonidipine, and nitrendipine were chosen on the basis of earlier reports and our preliminary studies.[19–22]

In the experiment with *R*(−)-efonidipine, dnNRSF-Tg mice were left untreated (control) or were treated for 20 weeks with the *R*(−)-isomer efonidipine (200 mg · kg^{-1} · d^{-1} PO). Acute myocardial infarction was induced in female C57BL/6 mice (age 8 to 12 weeks; weight 19 to 24 g) by ligation of the left coronary artery as described previously.[23] Beginning 1 day after the operation, mice were left untreated (control) or were treated for 30 days with efonidipine hydrochloride (200 mg · kg^{-1} · d^{-1}) or nitrendipine (60 mg · kg^{-1} · d^{-1}).

Efonidipine and *R*(−)-isomer efonidipine were supplied by Nissan Chemical Industries, Ltd (Tokyo, Japan). Nitrendipine was purchased from Wako Pure Chemical Industries, Ltd (Osaka, Japan).

Patch-Clamp Studies

Myocytes were dispersed by a method described previously.[24] To record T- and L-type Ca^{2+} currents, electrodes were filled with Cs^+-rich solution that contained (in mmol/L): 100 CsCl, 50 NMDG, 10 TEA, 5 MgATP, 5 HEPES, and 10 EGTA (pH 7.2 with CsOH). After establishment of the ruptured whole-cell patch configuration in normal Tyrode solution, the bathing solution was switched to Na^+-free solution. A stock solution of efonidipine 10 mmol/L in DMSO was diluted to the desired concentration with Na^+-free bathing solution (final concentration 10 μmol/L).

Intracardiac Electrophysiology

A 1.7F octapolar catheter (CIBer mouse EP, NuMe, Hopkinton, NY) inserted via the jugular vein was used to perform a standard electrophysiological study protocol as described previously.[14,25]

Statistical Analysis

Data are presented as mean±SEM. Survival was analyzed by the Kaplan-Meier method with the log-rank test. ANOVA with post hoc Student-Newman-Keuls tests was used for comparisons among groups. Values of $P<0.05$ were considered significant. Repeated-measures analyses with linear mixed-effects models were performed with data comprising repeated observations made over time. Data obtained from the 2-way factorial design were analyzed with the 2-way ANOVA.

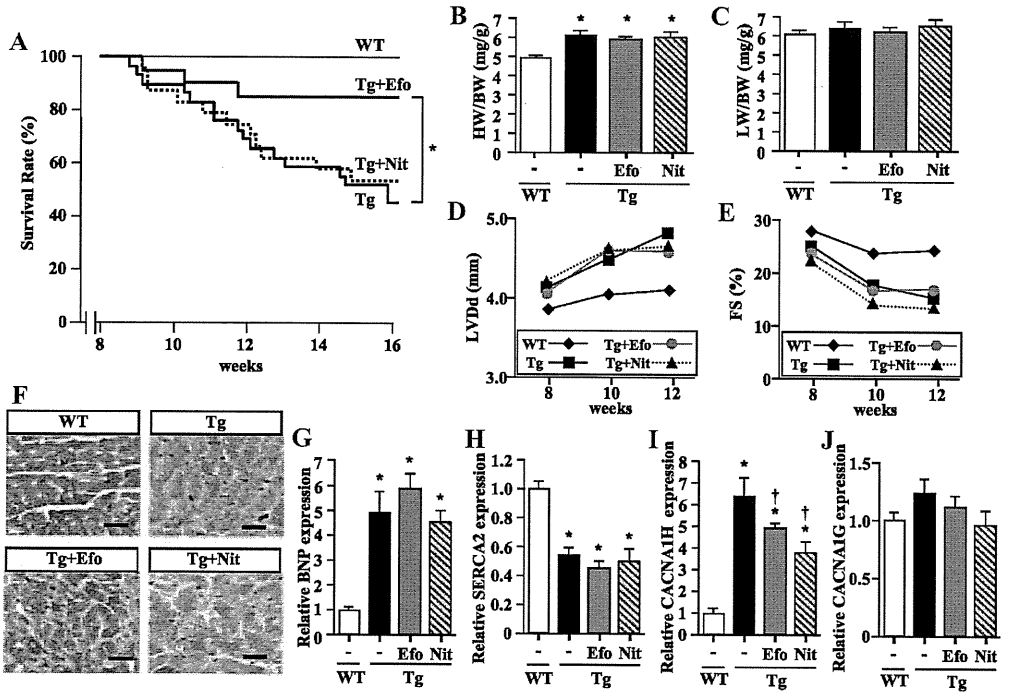

Figure 2. Efonidipine prolongs survival among dnNRSF-Tg mice. A, Kaplan-Meier survival curves for WT and dnNRSF-Tg (Tg) mice, with or without efonidipine (Efo) or nitrendipine (Nit), during the 7-week drug administration period (from 8 to 15 weeks of age). *$P<0.05$ (n=7 for WT, n=27 for Tg without drugs, n=19 for Tg with Efo, n=22 for Tg with Nit). B and C, heart weight–to–body weight (HW/BW) ratios (B) and lung weight–to–body weight (LW/BW) ratios (C) in 12-week-old WT and Tg mice, with or without Efo or Nit. *$P<0.05$ vs WT (n=10 for each group). D and E, Left ventricular diastolic dimension (LVDd; D) and % fractional shortening (FS; E), assessed echocardiographically in WT and Tg mice, with or without Efo or Nit, during a 4-week period beginning when the mice were 8 weeks of age (n=4 for WT, n=5 for Tg without drugs, n=6 for Tg with Efo, n=5 for Tg with Nit). The comparison of trends in LVDd and FS over time among Tg, Tg with Efo, and Tg with Nit, by repeated-measures analyses with linear mixed-effects models, showed no statistical significance (LVDd, $P=0.689$; FS, $P=0.735$). F, Histology of WT and dnNRSF-Tg hearts from 12-week-old mice treated with or without Efo or Nit. Hematoxylin-and-eosin staining; magnification ×400. Scale bars=20 μm. G–J, Relative levels of *BNP* (G), *SERCA2* (H), *CACNA1H* (I), and *CACNA1G* (J) mRNA expression in hearts from 12-week-old WT and Tg mice treated with or without Efo or Nit. *$P<0.05$ vs WT, †$P<0.05$ vs Tg without drugs (n=4 for WT, n=5 for Tg without drugs, n=4 for Tg with Efo, n=4 for Tg with Nit).

Results

Dual T- and L-Type Ca^{2+} Channel Blocker Efonidipine Improves Survival Among dnNRSF-Tg Mice

We previously showed that dnNRSF-Tg mice develop progressive cardiomyopathy and begin to die of ventricular tachyarrhythmias at ≈8 weeks of age.[14] In dnNRSF-Tg hearts, *CACNA1H*, the gene that encodes the T-type Ca^{2+} channel α-subunit and a transcriptional target of NRSF/REST, was upregulated, and there was a corresponding increase in $I_{Ca,T}$ amplitude in the isolated ventricular myocytes (Figure 1A through 1C).[14] By contrast, no $I_{Ca,T}$ were recorded in adult ventricular myocytes from wild-type littermate (WT) hearts (Figure 1A).[14] To determine the role played by T-type Ca^{2+} channels in the development of malignant arrhythmias and sudden death and to assess the potential therapeutic effect of T-type Ca^{2+} channel blockade in dnNRSF-Tg mice, we administered subpressor doses of efonidipine, a dual T- and L-type dihydropyridine Ca^{2+} channel blocker,[15,16] or nitrendipine, a more L-type-selective dihydropyridine Ca^{2+} channel blocker, to dnNRSF-Tg mice for 7 weeks, beginning when they were 8 weeks of age. Initially, we confirmed that efonidipine significantly blocked $I_{Ca,T}$ in ventricular myocytes from dnNRSF-Tg mice (Figure 1D and 1E). Consistent with previous reports, efonidipine also blocked $I_{Ca,L}$ in those cells (Figure 1D and 1E).[15,16] As shown in Figure 2A, efonidipine dramatically improved the survival rate among dnNRSF-Tg mice compared with mice treated with nitrendipine or control vehicle. We found that heart weight–to–body weight ratios and lung weight–to–body weight ratios did not differ among the control, efonidipine, and nitrendipine groups (Figure 2B and 2C). In addition, echocardiographic, hemodynamic, and histological analyses showed no significant differences among these 3 groups (Figure 2D, 2E, and 2F; Table). Consistent with these findings, there also was no significant difference in the expression of 2 cardiac stress marker genes, *BNP* and *SERCA2*, among the 3 groups (Figure 2G and 2H).[26,27] Both efonidipine and nitrendipine modestly reduced the increase in *CACNA1H* expression seen in dnNRSF-Tg hearts (Figure 2I), and the expression of *CACNA1G* did not significantly differ among WT and dnNRSF-Tg mice (Figure 2J). These data suggest that efonidipine directly suppresses sudden death in dnNRSF-Tg mice without significantly affecting cardiac structure or function.

Efonidipine Reduces Arrhythmogenicity in dnNRSF-Tg Mice

We next used a telemetric monitoring system to examine the effects of each drug on ECG parameters in dnNRSF-Tg mice. We found that only efonidipine significantly suppressed the

Table. Body Weight, Blood Pressure, and Hemodynamic Parameters in 12-Week-Old WT and dnNRSF-Tg Mice Treated With or Without Efonidipine or Nitrendipine

		dnNSF-Tg Mice		
	WT	Untreated	Treated With Efonidipine	Treated With Nitrendipine
Body weight, g	26.5±0.5	25.0±0.4*	24.8±0.6*	24.6±0.4*
Blood pressure, mm Hg	105.3±3.6	96.7±2.2*	94.4±3.8*	98.0±7.1*
Echocardiographic data				
LVDd, mm	4.1±0.4	4.8±0.2*	4.6±0.2*	4.6±0.2*
LVDs, mm	3.3±0.1	4.1±0.2*	3.8±0.1*	4.0±0.2*
FS, %	23.5±0.3	14.0±1.6*	17.0±0.6*	13.8±0.4*
IVS, mm	0.75±0.03	0.72±0.04	0.78±0.05	0.76±0.02
PW, mm	0.73±0.02	0.70±0.04	0.68±0.04	0.76±0.02
Hemodynamic data				
LVSP, mm Hg	112±3	107±3*	105±2*	103±3*
LVEDP, mm Hg	7.4±0.9	6.3±2.1	4.8±1.1	8.0±0.9
dP/dt, mm Hg/s	5430±150	4600±248*	4683±192*	4480±213*
−dP/dt, mm Hg/s	4400±435	3775±309	3833±158	3440±260
HR, bpm	452±39	415±20	419±36	428±26

LVDd indicates left ventricular diastolic dimension; LVDs, left ventricular systolic dimension; FS, fractional shortening; IVS, intraventricular septum wall thickness; PW, posterior wall thickness; LVSP, left ventricular systolic pressure; LVEDP, left ventricular end-diastolic pressure; and HR, heart rate.

Values are mean±SEM. Numbers of mice tested were as follows: Body weight, n=10 for each group; blood pressure, n=6 for WT mice, n=14 for dnNRSF-Tg mice without drugs, n=5 for dnNRSF-Tg mice treated with efonidipine, n=7 for dnNRSF-Tg mice treated with nitrendipine; echocardiographic data, n=4 for WT mice, n=5 for dnNRSF-Tg mice without drugs, n=6 for dnNRSF-Tg mice treated with efonidipine, n=5 for dnNRSF-Tg mice treated with nitrendipine; hemodynamic data, n=5 for WT mice, n=4 for dnNRSF-Tg mice without drugs, n=6 for dnNRSF-Tg mice treated with efonidipine, n=5 for dnNRSF-Tg mice treated with nitrendipine.

*$P<0.05$ vs WT mice.

number of premature ventricular contractions in dnNRSF-Tg hearts (Figure 3A). More importantly, it dramatically reduced the number of episodes of ventricular tachycardia (VT; Figure 3B).

We further assessed the effect of each drug on arrhythmogenicity in dnNRSF-Tg mice by performing an in vivo intracardiac electrophysiological analysis.[14,25] We found that control dnNRSF-Tg mice were highly susceptible to induction of VT, as reported previously[14] (Figure 3C and 3D), and that nitrendipine did not reduce that susceptibility (Figure 3D). By contrast, efonidipine significantly reduced the frequency of induced VT (Figure 3C and 3D). To confirm that inhibition of T-type Ca^{2+} currents is responsible for the suppression of arrhythmogenicity in dnNRSF-Tg hearts, we next treated dnNRSF-Tg mice with another dual T- and L-type Ca^{2+} channel blocker, mibefradil.[28] After 1 week of treatment with mibefradil or efonidipine, dnNRSF-Tg mice showed significantly reduced susceptibility to induced VT (Figure 3E).

We next examined the effects of long-term drug treatment on the electrophysiological properties of myocytes isolated from dnNRSF-Tg hearts. When we measured action potentials elicited in isolated ventricular myocytes from WT and dnNRSF-Tg hearts, we found that in the latter, the membrane potential was somewhat depolarized, and the action potential duration was increased (Figure 3F and 3G). Efonidipine, but not nitrendipine, significantly restored the resting membrane potential in dnNRSF-Tg myocytes (Figure 3F and 3G).

Efonidipine Improves Cardiac Autonomic Nervous System Function in dnNRSF-Tg Mice

A disturbance of autonomic nerve activity that leads to increased sympathetic nerve activity and reduced parasympathetic nerve activity is involved in the increased arrhythmogenicity seen in patients with chronic heart failure. Heart rate variability (HRV) is a widely accepted index of cardiac autonomic nervous system activity.[29] A previous frequency-domain analysis of HRV revealed that patients with severe heart failure show a progressive reduction in power in both the low-frequency and high-frequency ranges.[29,30] Moreover, the reduction in low-frequency power is a significant predictor of sudden cardiac death in patients with heart failure.[31,32]

T-type Ca^{2+} channels are normally expressed in neuronal and endocrine tissues, where they play an important role in mediating neurotransmitter release and in the secretion of various neurohumoral factors, including catecholamines.[33] Indeed, T-type Ca^{2+} channel blockade reportedly modulates autonomic activity.[34,35] With that in mind, we hypothesized that in addition to its direct effects on cardiac electrophysiological properties, T-type Ca^{2+} blockade reduces arrhythmogenicity by modulating autonomic nerve function. To test that idea, we used HRV as an index with which to evaluate cardiac autonomic function in WT and dnNRSF-Tg mice.[29] In mice, HRV predominantly correlates with parasympathetic activity.[36] Mice are nocturnal, so that for any given "day," the power in both the low- and high-frequency ranges was lower during the dark (night) phase, when the mice were more

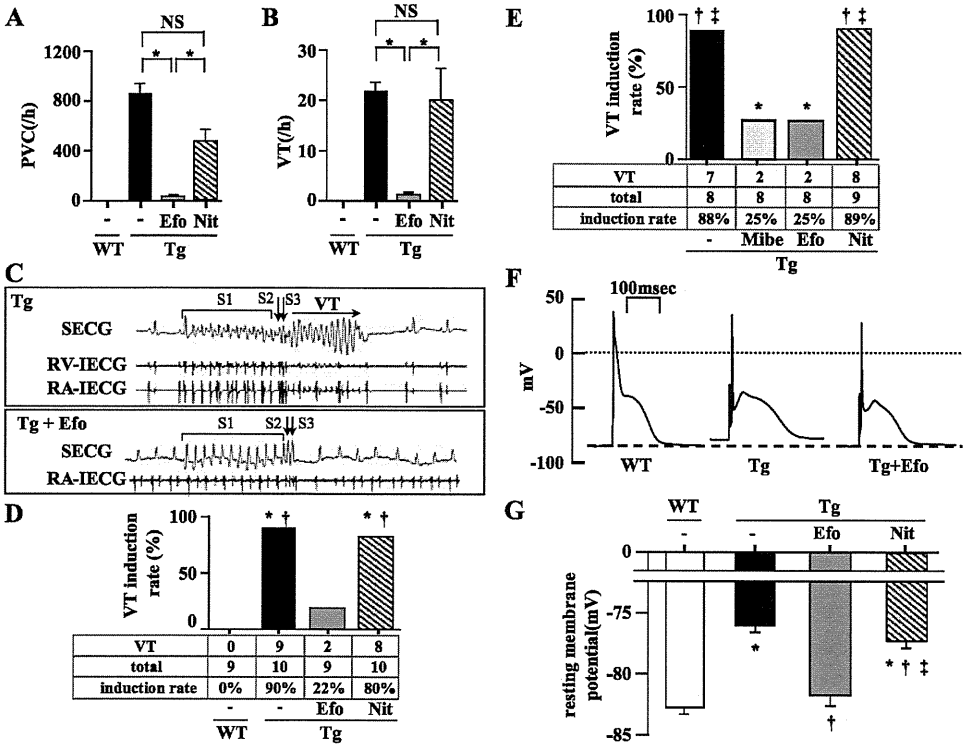

Figure 3. Efonidipine reduces arrhythmogenicity in dnNRSF-Tg hearts. A and B, Numbers of premature ventricular contractions (PVC; A) and VT (B) recorded with a telemetry system in WT and dnNRSF-Tg (Tg) mice treated with or without efonidipine (Efo) or nitrendipine (Nit). *$P<0.05$ (n=5 for WT, n=8 for Tg without drugs, n=7 for Tg with Efo, n=7 for Tg with Nit). C, Representative ECG traces from an in vivo electrophysiological study performed to evaluate the inducibility of VT in Tg hearts from mice treated with or without Efo. VT was induced in control hearts (upper panel) but not in those treated with efonidipine (Tg+Efo, lower panel). SECG indicates surface ECG; RV-IECG, intracardiac ECG (right ventricle); and RA-IECG, intracardiac ECG (right atrium). D, Frequency of mice with inducible VTs in Tg mice treated for 7 weeks with or without Efo or Nit. VT indicates number of mice with inducible VT; total, total number of mice tested. *$P<0.05$ vs WT, †$P<0.05$ vs Tg with Efo. E, Frequency of mice with inducible VTs in Tg mice treated for 1 week with or without mibefradil (Mibe), Efo, or Nit. VT indicates number of mice with inducible VT; total, total number of mice tested. *$P<0.05$ vs Tg, †$P<0.05$ vs Tg with Mibe; ‡$P<0.05$ vs Tg with Efo. F and G, Representative traces of action potentials (F) and averages of resting membrane potentials (G) recorded from isolated ventricular myocytes from 12-week-old WT and Tg mice treated with or without Efo. *$P<0.05$ vs WT, †$P<0.05$ vs control Tg, ‡$P<0.05$ vs Tg with Efo (n=12 for WT, n=12 for Tg without drugs, n=14 for Tg with Efo, n=18 for Tg with Nit).

active, than during the light (day) phase (online-only Data Supplement Figure IA and IB). In dnNRSF-Tg mice, the incidences of both premature ventricular contractions and VTs were much greater during the dark phase, which suggests the involvement of autonomic nerve activity in the generation of arrhythmias in these mice (online-only Data Supplement Figure IC and ID). In addition, the averages of both the low- and high-frequency powers over 24 hours in dnNRSF-Tg mice were markedly lower than in WT mice, which indicates a general reduction in parasympathetic activity in dnNRSF-Tg mice (Figure 4A, 4B, and 4C). Efonidipine dramatically increased the power in both the low- and high-frequency ranges of HRV in dnNRSF-Tg mice, whereas nitrendipine had little effect on HRV (Figure 4A, 4B, and 4C). We also found that urinary excretion of norepinephrine, which is indicative of the level of sympathetic nerve activity, was significantly higher in dnNRSF-Tg than in WT mice (Figure 5A). Moreover, the increased excretion of norepinephrine seen in dnNRSF-Tg mice was attenuated significantly only by efonidipine (Figure 5A).

We next evaluated the response of dnNRSF-Tg myocytes to catecholaminergic stimulation. We found that in the presence of isoproterenol 3 μmol/L, isolated ventricular myocytes from dnNRSF-Tg hearts showed early afterdepolarizations and spontaneous action potentials, whereas myocytes from WT hearts did not (Figure 5B, through 5D). In addition, systemic administration of isoproterenol induced VT more frequently in dnNRSF-Tg mice than in WT mice (Figure 5E). These data support our idea that abnormal autonomic nervous system balance, with decreased parasympathetic activity and increased sympathetic activity, facilitates arrhythmogenesis in dnNRSF-Tg mice. The increase in the frequency of isoproterenol-induced VT seen in dnNRSF-Tg mice was attenuated significantly by efonidipine but not by nitrendipine (Figure 5E). Thus, along with its direct effect, which reduces the vulnerability of the heart to arrhythmogenic stress (Figures 3D, 3E, and 5E), efonidipine also improves the cardiac autonomic nervous system balance, which further contributes to the suppression of lethal arrhythmias in dnNRSF-Tg mice.

R(−)-Efonidipine, a Highly Selective T-Type Ca^{2+} Channel Blocker, Dramatically Improves Survival Among dnNRSF-Tg Mice

Recently, *R*(−)-efonidipine was shown to be a specific blocker of T-type Ca^{2+} channels.[17,18] To further confirm the

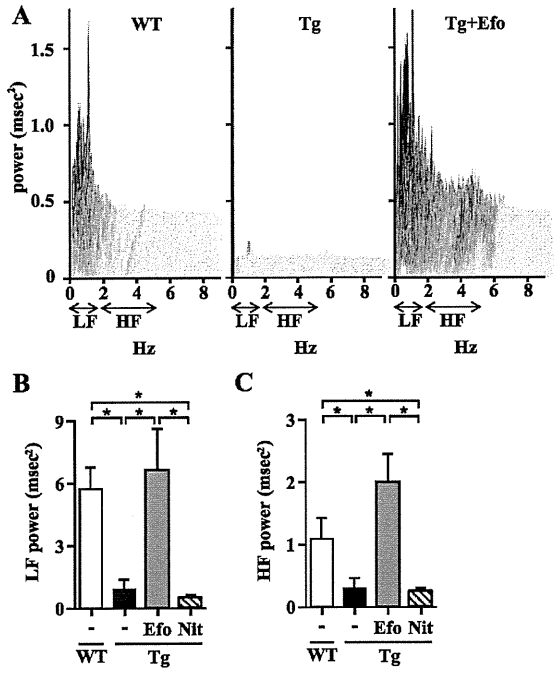

Figure 4. Efonidipine restores cardiac autonomic nervous system function in dnNRSF-Tg mice. A, Representative HRV data from 12-week-old WT and dnNRSF-Tg (Tg) mice treated with or without efonidipine (Efo). Low-frequency (LF) and high-frequency (HF) ranges are shown. B and C, Average power of the LF (B) and HF (C) components of HRV recorded over a 24-hour period in WT and Tg mice treated with or without Efo or nitrendipine (Nit). *P<0.05 (n=5 for WT, n=4 for Tg without drugs, n=4 for Tg with Efo, n=4 for Tg with Nit).

beneficial effects of T-type Ca^{2+} channel blockade in the prevention of sudden death in dnNRSF-Tg mice, we administered $R(-)$-efonidipine (200 mg · kg^{-1} · d^{-1} PO) to dnNRSF-Tg mice for 20 weeks. We found that $R(-)$-efonidipine did not significantly affect blood pressure, heart rate, cardiac structure, or systolic function in either WT or dnNRSF-Tg mice compared with vehicle (Figure 6A through 6E). By contrast, $R(-)$-efonidipine dramatically improved the survival rate among dnNRSF-Tg mice, which clearly suggests that T-type Ca^{2+} channel blockade prevents sudden death in dnNRSF-Tg mice (Figure 6F).

Efonidipine Reduces Sudden Death and Arrhythmogenicity in Mice With Acute Myocardial Infarction

Disturbance of cardiac autonomic nervous activity contributes to the incidence of arrhythmogenicity and mortality among patients with chronic heart failure due to nonischemic or ischemic cardiomyopathy, as well as among patients with acute myocardial infarction.[29] To test whether efonidipine can improve the survival rate among mice with a cardiomyopathy other than the nonischemic cardiomyopathy seen in dnNRSF-Tg mice, we administered efonidipine or nitrendipine to WT mice previously subjected to acute myocardial infarction. We found that efonidipine significantly reduced the incidence of sudden death during the subacute phase of myocardial infarction (Figure 7A), although blood pressure, cardiac systolic function, and cardiac structure were all similar in the control, efonidipine, and nitrendipine groups (Figure 7B through 7F). When we further assessed arrhythmogenicity among these mice, we found that control mice with myocardial infarction were highly susceptible to induction of VT and that efonidipine, but not nitrendipine, significantly reduced the frequency of induced VT among mice with myocardial infarction (Figure 7G; online-only Data Supplement Figure II).

Discussion

Ca^{2+} influx is involved in multiple cellular processes, including cell growth, differentiation, and death. In cardiac myocytes, Ca^{2+} influx plays important roles under both normal physiological and pathophysiological conditions. One of the major sources of Ca^{2+} influx in excitable cells is voltage-gated Ca^{2+} channels, which have been classified into several

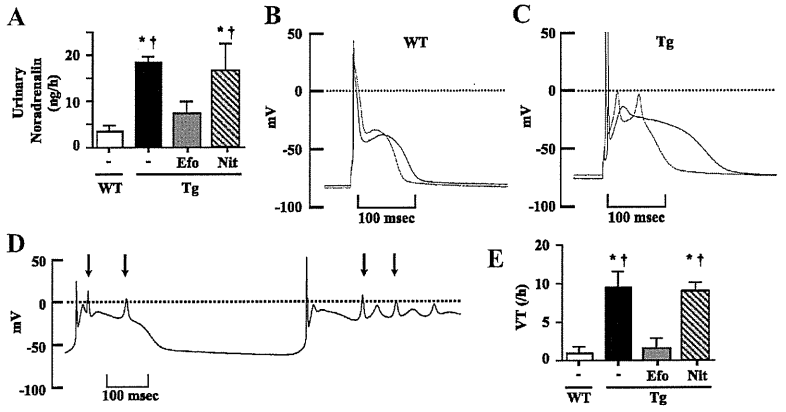

Figure 5. Catecholamine-induced ventricular arrhythmias in dnNRSF-Tg hearts. A, Urinary norepinephrine (noradrenalin) levels in WT and dnNRSF-Tg (Tg) mice treated with or without efonidipine (Efo) or nitrendipine (Nit). *P<0.05 vs WT, †P<0.05 vs Tg treated with Efo (n=4 for WT, n=6 for Tg without drugs, n=4 for Tg with Efo, n=4 for Tg with Nit). B and C, Representative tracings of action potentials recorded in the presence (red lines) or absence (black lines) of isoproterenol 3 μmol/L from ventricular myocytes isolated from WT (B) and Tg (C) hearts. D, Representative trace showing normal and induced spontaneous action potentials recorded in the presence of isoproterenol 3 μmol/L from ventricular myocytes isolated from Tg hearts. Arrows indicate induced spontaneous action potentials. E, Number of episodes of VT induced in 15 minutes after intraperitoneal administration of isoproterenol (20 μg) to WT or Tg mice treated with or without Efo or Nit. *P<0.05 vs WT, †P<0.05 vs Tg with Efo. Numbers of mice tested were as follows: WT=5, Tg without drugs=5, Tg with Efo=5, Tg with Nit=4.

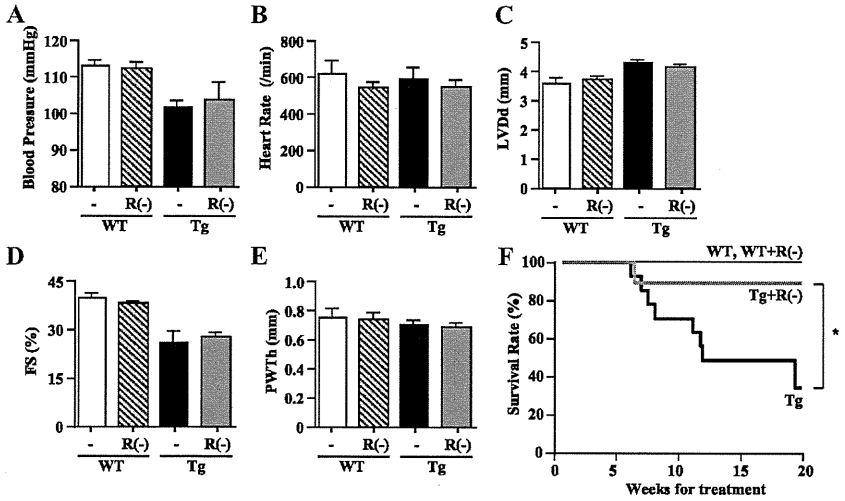

Figure 6. *R*(−)-efonidipine prolongs survival among dnNRSF-Tg mice. A and B, Blood pressures (A) and heart rates (B) in 12-week-old WT and dnNRSF-Tg (Tg) mice treated for 4 weeks with or without *R*(−)-efonidipine [*R*(−)]; n=2 for WT, n=3 for WT with *R*(−), n=5 for Tg, n=4 for Tg with *R*(−). C, D, and E, Left ventricular diastolic dimension (LVDd; C), % fractional shortening (FS; D), and posterior wall thickness (PWTh; E) assessed echocardiographically in 12-week-old WT and Tg mice treated for 4 weeks with or without *R*(−) [n=2 for WT, n=3 for WT with *R*(−), n=4 for Tg and Tg with *R*(−)]. Two-way ANOVA revealed that Tg mice showed decreased blood pressure and enlarged LVDd compared with WT, and *R*(−) had no effect on blood pressure, heart rate, or echocardiographic data. No mice status/medication status interaction was observed [in A, $P<0.001$ between WT and Tg, $P=0.569$ between without and with *R*(−), interaction $P=0.267$; in B, $P<0.725$ between WT and Tg, $P=0.216$ between without and with *R*(−), interaction $P=0.179$; in C, $P<0.001$ between WT and Tg, $P=0.710$ between without and with *R*(−), interaction $P=0.131$; in D, $P<0.001$ between WT and Tg, $P=0.919$ between without and with *R*(−), interaction $P=0.457$; in E, $P=0.304$ between WT and Tg, $P=0.664$ between without and with *R*(−), interaction $P=0.950$]. F, Kaplan-Meier survival curves for WT and Tg mice with or without *R*(−) during a 20-week drug administration period beginning at 8 weeks of age. *$P<0.05$ [n=6 for WT, n=3 for WT with *R*(−), n=13 for Tg, n=9 for Tg with *R*(−)].

types: L (long lasting), T (transient), N (neuronal), P/Q (Purkinje), and R (residual-drug resistant). Generally, cardiac myocytes express only the L and T types.[37] L-type Ca^{2+} channels predominate in mature cardiac myocytes and are crucially involved in excitation-contraction coupling.[37] T-type Ca^{2+} channels are expressed abundantly in embryonic ventricular myocytes.[4,5] After birth, however, expression of T-type Ca^{2+} channels is downregulated in ventricular myocytes,[4,5] so that they are restricted to the conduction system,[3,5] where they modulate pacemaking activities.[3,38] But under conditions of cardiac hypertrophy and heart failure, T-type Ca^{2+} channels are reexpressed in ventricular myocytes,[4,6–8]

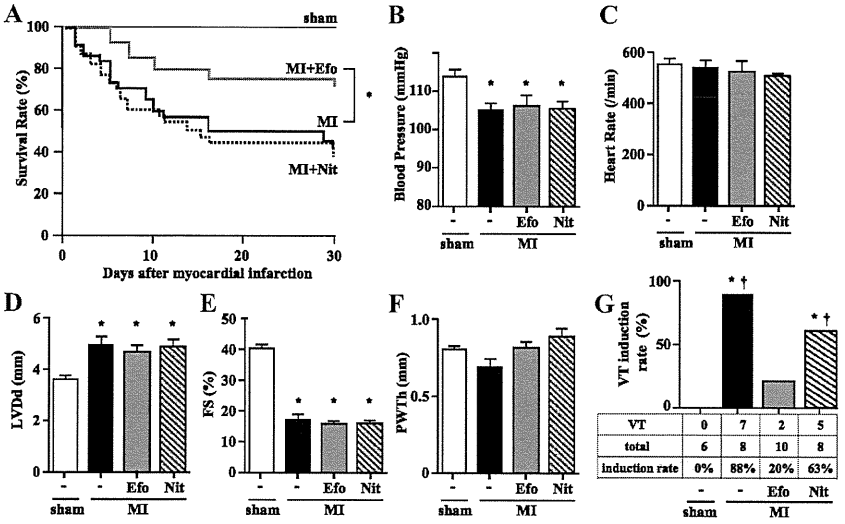

Figure 7. Efonidipine prevented sudden death among mice with acute myocardial infarction. A, Kaplan-Meier survival curves for sham-operated mice (sham) and mice with myocardial infarction (MI) treated for 30 days with or without efonidipine (Efo) or nitrendipine (Nit) beginning at 8 to 12 weeks of age. *$P<0.05$ (n=12 for sham, n=39 for MI, n=29 for MI with Efo, and n=29 for MI with Nit). B and C, Blood pressures (B) and heart rates (C) in sham and MI mice treated for 4 weeks with or without Efo or Nit. *$P<0.05$ vs sham (n=7 in each group). D, E, and F, Left ventricular diastolic dimension (LVDd; D), % fractional shortening (FS; E), and posterior wall thickness (PWTh; F) assessed echocardiographically in sham and MI mice treated for 4 weeks with or without Efo or Nit. *$P<0.05$ vs sham (n=10 for sham, n=6 for MI, n=10 for MI with Efo, and n=8 for MI with Nit). G, Frequency of mice with inducible VT in sham and MI mice treated for 4 weeks with or without Efo or Nit are shown. VT indicates number of mice with inducible VT; total, total number of mice tested. *$P<0.05$ vs WT, †$P<0.05$ vs MI with Efo.

and they are thought to be involved in the altered cardiac function and arrhythmogenicity seen in the diseased myocardium.[2,3] Consistent with that idea, the dual T- and L-type Ca^{2+} channel blocker mibefradil attenuates the pathological processes seen in some animal models of cardiac disease.[10,11,39] Moreover, it was recently reported that genetic deletion of *CACNA1H* results in resistance to pathological cardiac hypertrophy.[9] Nonetheless, the effect of T-type Ca^{2+} channel blockade on the incidence of malignant arrhythmias and sudden death remains unknown.

In the present study, we demonstrated that the dual T- and L-type Ca^{2+} channel blocker efonidipine prevents the sudden death and arrhythmogenicity otherwise seen in dnNRSF-Tg mice, whereas nitrendipine, a selective L-type Ca^{2+} channel blocker, does not. Suppression of arrhythmogenicity also was observed when dnNRSF-Tg mice were treated with mibefradil. Although the doses of nitrendipine used in the present studies (20 and 60 mg/kg) did not significantly affect blood pressure in dnNRSF-Tg mice, those doses previously were shown to effectively block L-type Ca^{2+} channels in mice.[19] We also observed that treatment of db/db mice, a mouse model of type 2 diabetes–associated hypertension,[40] with nitrendipine 10 mg $\cdot$ kg^{-1} $\cdot$ d^{-1} for 8 days significantly reduced their elevated blood pressure (unpublished observation). These results clearly demonstrate that blockade of T-type Ca^{2+} channels, not L-type Ca^{2+} channels, mediates the effects of efonidipine and mibefradil on dnNRSF-Tg mice, although there is still the possibility that unknown effects of efonidipine and mibefradil on other currents are responsible. Furthermore, *R*(−)-efonidipine, a recently identified specific blocker of T-type Ca^{2+} channels,[17,18] dramatically improved the survival rate among dnNRSF-Tg mice, which strongly supports the notion that T-type Ca^{2+} channels play a key role in mediating the lethal arrhythmias seen in this animal model. In addition, efonidipine, but not nitrendipine, also reduced the incidence of sudden death and arrhythmias among mice with acute myocardial infarction. Collectively, the lines of evidence summarized above demonstrate that T-type Ca^{2+} channel blockade prevents sudden death and malignant arrhythmias in mice with heart failure caused by either nonischemic or ischemic myocardial injury.

Abnormalities in atrial and ventricular electrophysiology are well-recognized contributors to arrhythmogenesis in diseased human hearts.[1] In dnNRSF-Tg mice, the action potential is prolonged, and the resting membrane potential is depolarized, which is consistent with features observed in failing human hearts.[1] Notably, efonidipine significantly restored the resting membrane potential in ventricular myocytes from dnNRSF-Tg mice. Given that membrane depolarization can enhance arrhythmogenicity by inducing triggered activity mediated by early afterdepolarizations or delayed afterdepolarizations and by increasing automaticity,[1] restoration of the resting membrane potential is likely 1 of the mechanisms by which efonidipine prevents ventricular arrhythmias and sudden cardiac death in dnNRSF-Tg mice. Although we still do not fully understand the mechanism by which T-type Ca^{2+} channel blockade restores the membrane potential in dnNRSF-Tg cardiomyocytes, the activation and availability of $I_{Ca,T}$ overlap at membrane potentials in the range of −60 to −30 mV, which could contribute to a pathological Ca^{2+} leak into cells during diastole.[3] It was recently reported that elevation of diastolic Ca^{2+} reduced the amplitude of I_{K1}, which is a critical determinant of resting membrane potential in ventricular myocytes.[41] In fact, the amplitude of I_{K1} was reduced significantly in dnNRSF-Tg ventricular myocytes (unpublished observation). It was also recently shown with mice lacking *CACNA1H* that the α1H T-type Ca^{2+} channel plays a pivotal role in the induction of pathological calcineurin/nuclear factor–activated T cell signaling, which increases susceptibility to arrhythmias.[9,42,43] T-type Ca^{2+} channel blockade may correct abnormalities in ventricular electrophysiology in part by inhibiting these pathological signaling pathways.

Disturbance of cardiac autonomic nervous activity that leads to increased sympathetic nerve activity and decreased parasympathetic nerve activity contributes to the increased arrhythmogenicity seen in patients with chronic heart failure.[44] HRV analysis is widely used to assess autonomic nerve function in the heart and has been shown to correlate with the prognosis of patients with heart failure.[31,32] In the present study, efonidipine clearly reversed the altered HRV seen in dnNRSF-Tg mice. L-type Ca^{2+} channel blockers generally enhance sympathetic nerve activity and reduce parasympathetic nerve activity.[34,45] By contrast, efonidipine appears to have the opposite effects on autonomic nerve activity. In a previous study performed in mildly to moderately hypertensive patients, mibefradil enhanced parasympathetic nervous activity.[34] Similarly, in another study of hypertensive patients, efonidipine improved the disturbed balance in autonomic nerve activity in the heart.[35] The involvement of T-type Ca^{2+} channels in the release of neurotransmitters, including catecholamines, from neuronal and endocrine cells may account for the effects of T-type Ca^{2+} channel blockade on autonomic nerve activity.[33] Consistent with that idea, we observed in the present study that efonidipine significantly reduces the increase in urinary norepinephrine excretion otherwise seen in dnNRSF-Tg mice. Thus, along with its direct effects on the electrophysiology of ventricular myocytes, the effects of efonidipine on cardiac autonomic function likely contribute to the prevention of malignant arrhythmias and sudden death in dnNRSF-Tg mice. There is also the possibility that correcting the balance between sympathetic and parasympathetic nerve activity affects the electrophysiological properties of ventricular myocytes. The present results showing that efonidipine reduces the incidence of sudden death among mice with acute myocardial infarction further support the idea that correcting the balance in cardiac autonomic nerve activity through blockade of T-type Ca^{2+} channels contributes to the prevention of malignant arrhythmias and sudden death by efonidipine, because disturbances in cardiac autonomic nervous activity are associated with sudden death in patients with acute myocardial infarction.[46,47]

Mibefradil was approved for use in the treatment of hypertension, angina pectoris, and congestive heart failure in 1997 but was withdrawn from the market because of an unexpected side effect unrelated to the T-type Ca^{2+} channel blockade: It inhibited cytochrome p450s, thereby causing negative drug-drug interactions.[2] On the other hand, efonidip-

ine has been used to treat hypertension for several years in Japan, and no such severe side effects have yet been identified. Although further investigation is necessary, we suggest that efonidipine or some other T-type Ca^{2+} channel blockers, including the *R*(−)-isomer efonidipine, may be clinically useful for the prevention of sudden arrhythmic death in patients with heart failure.

Acknowledgments

We thank Yukari Kubo for her excellent secretarial work.

Sources of Funding

This research was supported by a grant-in-aid for scientific research from the Japan Society for the Promotion of Science (to Dr Kuwahara., Dr Harada, and Dr Nakao.), and grants from the Japanese Ministry of Health, Labor and Welfare (to Dr Nakao) and from the Japan Heart Foundation/Pfizer Pharmaceuticals Inc Grant on Cardiovascular Disease Research, the Japan Heart Foundation/ Novartis Grant for Research Award on Molecular and Cellular Cardiology, the Mochida Memorial Foundation for Medical and Pharmaceutical Research, the Uehara Memorial Foundation, the Ichiro Kanehara Foundation, the Astellas Foundation for Research on Metabolic Disorders, the Mitsubishi Foundation, the Suzuken Memorial Foundation, the Takeda Medical Research Foundation, and the Kanae Foundation for the Promotion of Medical Science (to Dr Kuwahara).

Disclosures

None.

References

1. Tomaselli GF, Marbán E. Electrophysiological remodeling in hypertrophy and heart failure. *Cardiovasc Res.* 1999;42:270–283.
2. Clozel JP, Ertel EA, Ertel SI. Voltage-gated T-type Ca^{2+} channels and heart failure. *Proc Assoc Am Physicians.* 1999;111:429–437.
3. Vassort G, Talavera K, Alvarez JL. Role of T-type Ca^{2+} channels in the heart. *Cell Calcium.* 2006;40:205–220.
4. Yasui K, Niwa N, Takemura H, Opthof T, Muto T, Horiba M, Shimizu A, Lee JK, Honjo H, Kamiya K, Kodama I. Pathophysiological significance of T-type Ca^{2+} channels: expression of T-type Ca^{2+} channels in fetal and diseased heart. *J Pharmacol Sci.* 2005;99:205–210.
5. Niwa N, Yasui K, Opthof T, Takemura H, Shimizu A, Horiba M, Lee JK, Honjo H, Kamiya K, Kodama I. Cav3.2 subunit underlies the functional T-type Ca^{2+} channel in murine hearts during the embryonic period. *Am J Physiol Heart Circ Physiol.* 2004;286:H2257–H2263.
6. Nuss HB, Houser SR. T-type Ca^{2+} current is expressed in hypertrophied adult feline left ventricular myocytes. *Circ Res.* 1993;73:777–782.
7. Sen L, Smith TW. T-type Ca^{2+} channels are abnormal in genetically determined cardiomyopathic hamster hearts. *Circ Res.* 1994;75:149–155.
8. Martinez ML, Heredia MP, Delgado C. Expression of T-type Ca(2+) channels in ventricular cells from hypertrophied rat hearts. *J Mol Cell Cardiol.* 1999;31:1617–1625.
9. Chiang CS, Huang CH, Chieng H, Chang YT, Chang D, Chen JJ, Chen YC, Chen YH, Shin HS, Campbell KP, Chen CC. The Ca (v) 3.2 T-type Ca(2+) channel is required for pressure overload-induced cardiac hypertrophy in mice. *Circ Res.* 2009;104:522–530.
10. Villame J, Massicotte J, Jasmin G, Dumont L. Effects of mibefradil, a T- and L-type calcium channel blocker, on cardiac remodeling in the UM-X7.1 cardiomyopathic hamster. *Cardiovasc Drugs Ther.* 2001;15: 41–48.
11. Sandmann S, Min JY, Meissner A, Unger T. Effects of the calcium channel antagonist mibefradil on haemodynamic parameters and myocardial Ca(2+)-handling in infarct-induced heart failure in rats. *Cardiovasc Res.* 1999;44:67–80.
12. Mulder P, Richard V, Compagnon P, Henry JP, Lallemand F, Clozel JP, Koen R, Mace B, Thuillez C. Increased survival after long-term treatment with mibefradil, a selective T-channel calcium antagonist, in heart failure. *J Am Coll Cardiol.* 1997;29:416–421.
13. Kuwahara K, Saito Y, Ogawa E, Takahashi N, Nakagawa Y, Naruse Y, Harada M, Hamanaka I, Izumi T, Miyamoto Y, Kishimoto I, Kawakami R, Nakanishi M, Mori N, Nakao K. The neuron-restrictive silencer element-neuron-restrictive silencer factor system regulates basal and endothelin 1-inducible atrial natriuretic peptide gene expression in ventricular myocytes. *Mol Cell Biol.* 2001;21:2085–2097.
14. Kuwahara K, Saito Y, Takano M, Arai Y, Yasuno S, Nakagawa Y, Takahashi N, Adachi Y, Takemura G, Horie M, Miyamoto Y, Morisaki T, Kuratomi S, Noma A, Fujiwara H, Yoshimasa Y, Kinoshita H, Kawakami R, Kishimoto I, Nakanishi M, Usami S, Saito Y, Harada M, Nakao K. NRSF regulates the fetal cardiac gene program and maintains normal cardiac structure and function. *EMBO J.* 2003;22:6310–6321.
15. Masumiya H, Shijuku T, Tanaka H, Shigenobu K. Inhibition of myocardial L- and T-type Ca^{2+} currents by efonidipine: possible mechanism for its chronotropic effect. *Eur J Pharmacol.* 1998;349:351–357.
16. Horiba M, Muto T, Ueda N, Opthof T, Miwa K, Hojo M, Lee JK, Kamiya K, Kodama I, Yasui K. T-type Ca^{2+} channel blockers prevent cardiac cell hypertrophy through an inhibition of calcineurin-NFAT3 activation as well as L-type Ca^{2+} channel blockers. *Life Sci.* 2008;82:554–560.
17. Tanaka H, Komikado C, Shimada H, Takeda K, Namekata I, Kawanishi T, Shigenobu K. The R(-)-enantiomer of efonidipine blocks T-type but not L-type calcium current in guinea pig ventricular myocardium. *J Pharmacol Sci.* 2004;96:499–501.
18. Furukawa T, Miura R, Honda M, Kamiya N, Mori Y, Takeshita S, Isshiki T, Nukada T. Identification of R(-)-isomer of efonidipine as a selective blocker of T-type Ca^{2+} channels. *Br J Pharmacol.* 2004;143:1050–1057.
19. Jinnah HA, Yitta S, Drew T, Kim BS, Visser JE, Rothstein JD. Calcium channel activation and self-biting in mice. *Proc Natl Acad Sci U S A.* 1999;96:15228–15232.
20. Shudo C, Masuda Y, Sugita H, Tamura T, Furukawa S, Hayashi K, Hirata H, Shikada K, Tanaka S, Tomita K. Effects of efonidipine, nicardipine and captopril on proteinuria in aged spontaneously hypertensive rats. *Arzneimittelforschung.* 1996;46:852–854.
21. Furukawa T, Nukada T, Miura R, Ooga K, Honda M, Watanabe S, Koganesawa S, Isshiki T. Differential blocking action of dihydropyridine Ca^{2+} antagonists on a T-type Ca^{2+} channel (alpha1G) expressed in Xenopus oocytes. *J Cardiovasc Pharmacol.* 2005;45:241–246.
22. Yokoyama U, Minamisawa S, Adachi-Akahane S, Akaike T, Naguro I, Funakoshi K, Iwamoto M, Nakagome M, Uemura N, Hori H, Yokota S, Ishikawa Y. Multiple transcripts of Ca^{2+} channel alpha1-subunits and a novel spliced variant of the alpha1C-subunit in rat ductus arteriosus. *Am J Physiol Heart Circ Physiol.* 2006;290:H1660–H1670.
23. Kawakami R, Saito Y, Kishimoto I, Harada M, Kuwahara K, Takahashi N, Nakagawa Y, Nakanishi M, Tanimoto K, Usami S, Yasuno S, Kinoshita H, Chusho H, Tamura N, Ogawa Y, Nakao K. Overexpression of brain natriuretic peptide facilitates neutrophil infiltration and cardiac matrix metalloproteinase-9 expression after acute myocardial infarction. *Circulation.* 2004;110:3306–3312.
24. Shioya T. A simple technique for isolating healthy heart cells from mouse models. *J Physiol Sci.* 2007;57:327–335.
25. Gehrmann J, Berul CI. Cardiac electrophysiology in genetically engineered mice. *J Cardiovasc Electrophysiol.* 2000;11:354–368.
26. Mukoyama M, Nakao K, Hosoda K, Suga S, Saito Y, Ogawa Y, Shirakami G, Jougasaki M, Obata K, Yasue H. Brain natriuretic peptide as a novel cardiac hormone in humans: evidence for an exquisite dual natriuretic peptide system, atrial natriuretic peptide and brain natriuretic peptide. *J Clin Invest.* 1991;87:1402–1412.
27. Nakagawa O, Ogawa Y, Itoh H, Suga S, Komatsu Y, Kishimoto I, Nishino K, Yoshimasa T, Nakao K. Rapid transcriptional activation and early mRNA turnover of brain natriuretic peptide in cardiocyte hypertrophy: evidence for brain natriuretic peptide as an "emergency" cardiac hormone against ventricular overload. *J Clin Invest.* 1995;96:1280–1287.
28. Leuranguer V, Mangoni ME, Nargeot J, Richard S. Inhibition of T-type and L-type calcium channels by mibefradil: physiologic and pharmacologic bases of cardiovascular effects. *J Cardiovasc Pharmacol.* 2001; 37:649–661.
29. Task Force of the European Society of Cardiology and the North American Society of Pacing and Electrophysiology. Heart rate variability: standards of measurement, physiological interpretation and clinical use. *Circulation.* 1996;93:1043–1065.
30. Guzzetti S, Cogliati C, Turiel M, Crema C, Lombardi F, Malliani A. Sympathetic predominance followed by functional denervation in the progression of chronic heart failure. *Eur Heart J.* 1995;16:1100–1107.
31. La Rovere MT, Pinna GD, Maestri R, Mortara A, Capomolla S, Febo O, Ferrari R, Franchini M, Gnemmi M, Opasich C, Riccardi PG, Traversi E, Cobelli F. Short-term heart rate variability strongly predicts sudden

cardiac death in chronic heart failure patients. *Circulation.* 2003;107: 565–570.
32. Sandercock GR, Brodie DA. The role of heart rate variability in prognosis for different modes of death in chronic heart failure. *Pacing Clin Electrophysiol.* 2006;29:892–904.
33. Carbone E, Giancippoli A, Marcantoni A, Guido D, Carabelli V. A new role for T-type channels in fast "low-threshold" exocytosis. *Cell Calcium.* 2006;40:147–154.
34. Pellizzer AM, Kamen PW, Esler MD, Lim S, Krum H. Comparative effects of mibefradil and nifedipine gastrointestinal transport system on autonomic function in patients with mild to moderate essential hypertension. *J Hypertens.* 2001;19:279–285.
35. Harada K, Nomura M, Nishikado A, Uehara K, Nakaya Y, Ito S. Clinical efficacy of efonidipine hydrochloride, a T-type calcium channel inhibitor, on sympathetic activities. *Circ J.* 2003;67:139–145.
36. Just A, Faulhaber J, Ehmke H. Autonomic cardiovascular control in conscious mice. *Am J Physiol Regul Integr Comp Physiol.* 2000;279: R2214–R2221.
37. Bers DM. Cardiac excitation-contraction coupling. *Nature.* 2002;415: 198–205.
38. Huser J, Blatter LA, Lipsius SL. Intracellular Ca^{2+} release contributes to automaticity in cat atrial pacemaker cells. *J Physiol.* 2000;524(part 2):415–422.
39. Sandmann S, Bohle RM, Dreyer T, Unger T. The T-type calcium channel blocker mibefradil reduced interstitial and perivascular fibrosis and improved hemodynamic parameters in myocardial infarction-induced cardiac failure in rats. *Virchows Arch.* 2000;436:147–157.
40. Su W, Guo Z, Randall DC, Cassis L, Brown DR, Gong MC. Hypertension and disrupted blood pressure circadian rhythm in type 2 diabetic db/db mice. *Am J Physiol Heart Circ Physiol.* 2008;295:H1634–H1641.
41. Fauconnier J, Lacampagne A, Rauzier JM, Vassort G, Richard S. Ca^{2+}-dependent reduction of I_{K1} in rat ventricular cells: a novel paradigm for arrhythmia in heart failure? *Cardiovasc Res.* 2005;68:204–212.
42. Dong D, Duan Y, Guo J, Roach DE, Swirp SL, Wang L, Lees-Miller JP, Sheldon RS, Molkentin JD, Duff HJ. Overexpression of calcineurin in mouse causes sudden cardiac death associated with decreased density of K+ channels. *Cardiovasc Res.* 2003;57:320–332.
43. Khoo MS, Li J, Singh MV, Yang Y, Kannankeril P, Wu Y, Grueter CE, Guan X, Oddis CV, Zhang R, Mendes L, Ni G, Madu EC, Yang J, Bass M, Gomez RJ, Wadzinski BE, Olson EN, Colbran RJ, Anderson ME. Death, cardiac dysfunction, and arrhythmias are increased by calmodulin kinase II in calcineurin cardiomyopathy. *Circulation.* 2006;114: 1352–1359.
44. Anderson KP. Sympathetic nervous system activity and ventricular tachyarrhythmias: recent advances. *Ann Noninvasive Electrocardiol.* 2003;8:75–89.
45. Minami J, Ishimitsu T, Kawano Y, Matsuoka H. Effects of amlodipine and nifedipine retard on autonomic nerve activity in hypertensive patients. *Clin Exp Pharmacol Physiol.* 1998;25:572–576.
46. Ewing DJ. Heart rate variability: an important new risk factor in patients following myocardial infarction. *Clin Cardiol.* 1991;14:683–685.
47. Weiss JN, Nademanee K, Stevenson WG, Singh B. Ventricular arrhythmias in ischemic heart disease. *Ann Intern Med.* 1991;114:784–797.

CLINICAL PERSPECTIVE

Despite recent progress in nonpharmacological therapy, pharmacological interventions for the treatment and prevention of lethal arrhythmias associated with heart failure remain limited. In this study, we used mouse models of ischemic and nonischemic cardiomyopathy to show that T-type Ca^{2+} channel blockade diminishes arrhythmogenicity and prevents sudden death in heart failure. The dual T- and L-type Ca^{2+} channel blocker mibefradil was withdrawn from the market because of an unexpected side effect unrelated to the T-type Ca^{2+} channel blockade: It inhibited cytochrome p450s, thereby causing negative drug-drug interactions. Another dual T- and L-type Ca^{2+} channel blocker, efonidipine, which we used in this study, has been used in Japan for several years to treat hypertension, and no severe side effects have yet been identified. Although further investigation is necessary, our results suggest that efonidipine and perhaps other T-type Ca^{2+} channel blockers, especially selective T-type Ca^{2+} channel blockers such as the $R(-)$-isomer efonidipine, may be clinically useful for the prevention of lethal arrhythmias and sudden death in patients with heart failure.

www.nature.com/clinicalpractice/endmet

Adiposcience and adipotoxicity

Kazuwa Nakao

Traditionally, adipose tissue was viewed as a rather inert organ that functioned solely as a fat storage depot. However, this tissue is now recognized as a bona fide endocrine organ that has the ability to secret numerous adipokines, including leptin.

Excess storage of fat in adipose tissue (i.e. obesity) is accompanied by ectopic lipid deposition in nonadipose tissues, such as the liver, skeletal muscles and pancreas. The negative effects of ectopic lipid deposition on glucose metabolism have been proposed to reflect a state of 'lipotoxicity', in which leptin is implicated as an antilipotoxic hormone. Over the past decade, evidence has accumulated that the adipose tissue has multiple functions in both normal physiology and disease. These functions are affected by changes in the adipose-tissue mass and/or the distribution of fat in subcutaneous and visceral adipose tissues. These changes result in dynamic alteration of adipokine production that reflect the severity of obesity, chronic inflammation with the infiltration of macrophages, leptin resistance, and altered autonomic nervous function, in addition to insulin resistance and lipotoxicity. I, therefore, propose the term 'adipotoxicity' to describe the negative effects associated with obesity. Adipotoxicity can be defined as the sum of the negative effects associated with storage of excess fat in adipose tissue on obesity-related clinical features, such as diabetes mellitus and arteriosclerosis. As a consequence, the metabolic syndrome—an obesity-related cluster of diabetes mellitus, dyslipidemia and hypertension—should be studied from a comprehensive viewpoint that is based on the concept of adipotoxicity.

Detailed comparisons of obesity and generalized lipodystrophy (i.e. lack of adipose tissue) have contributed substantially to our understanding of adipotoxicity. In particular, the dramatic effects of leptin-replacement therapy on patients with lipodystrophy disclosed subtle functions of the adipose tissue, and became the paradigm used to elucidate the mechanisms of adipotoxicity. We should, however, remember that our current understanding of the function of adipose tissue is far from complete. Further studies on adipotoxicity will hopefully provide a new strategy that we can exploit to prevent and treat obesity and the metabolic syndrome.

...further studies on adipotoxicity will hopefully provide a new strategy that we can exploit to prevent and treat obesity...

Interpretation of the results of different studies that focus on obesity can be hampered by use of the misleading prefixes 'lipo' and 'adipo'. For example, lipogenesis is used to describe the metabolic formation of lipid, whereas adipogenesis refers to the differentiation of preadipocytes into mature adipocytes, the main function of which is to store fat. Of course, lipogenesis and adipogenesis are closely linked biological processes. Furthermore, a key aim of the study of obesity is to understand the significance of the storage of excess fat in the adipose tissue. I feel it is appropriate, then, to coin the term 'adiposcience' to describe studies that aim to evaluate the relationship between adipogenesis and obesity. The definition of adiposcience might also be extended to cover other aspects of metabolism, from appetite regulation to energy expenditure, as well as their mechanisms of action on the adipose tissue.

The prevalence of obesity and its comorbidities has now reached pandemic proportions. Indeed, the main theme of the 13th International Congress of Endocrinology (held during 8–12 November 2008 in Rio de Janeiro) was obesity and the metabolic syndrome. When the Congress reconvenes in Kyoto in March 2010, however, the concepts of adiposcience and adipotoxicity clearly should be at the forefront of our discussions.

K Nakao is the Chairman of the Department of Medicine and Clinical Science at Kyoto University Graduate School of Medicine, Kyoto, Japan.

Competing interests
The author declared no competing interests.

www.nature.com/clinicalpractice
doi:10.1038/ncpendmet1052

FEBS Letters 583 (2009) 1029–1033

ELSEVIER

FEBS Letters

journal homepage: www.FEBSLetters.org

Adipogenic differentiation of human induced pluripotent stem cells: Comparison with that of human embryonic stem cells

Daisuke Taura [a,1], Michio Noguchi [a,1], Masakatsu Sone [a,*], Kiminori Hosoda [a,*], Eisaku Mori [a], Yohei Okada [b], Kazutoshi Takahashi [c,d], Koichiro Homma [a,e], Naofumi Oyamada [a], Megumi Inuzuka [a], Takuhiro Sonoyama [a], Ken Ebihara [a], Naohisa Tamura [a], Hiroshi Itoh [e], Hirofumi Suemori [f], Norio Nakatsuji [g,h], Hideyuki Okano [b], Shinya Yamanaka [c,d], Kazuwa Nakao [a]

[a] Department of Medicine and Clinical Science, Kyoto University Graduate School of Medicine, 54 Shogoin Kawahara-cho, Sakyo-ku, Kyoto 606-8507, Japan
[b] Department of Physiology, Keio University, School of Medicine, Tokyo, Japan
[c] Department of Stem Cell Biology, Institute for Frontier Medical Sciences, Kyoto University, Kyoto, Japan
[d] Center for iPS Cell Research and Application (CiRA), Institute for Integrated Cell-Material Sciences, Kyoto, Japan
[e] Department of Internal Medicine, Keio University School of Medicine, Tokyo, Japan
[f] Laboratory of Embryonic Stem Cell Research, Stem Cell Research Center, Institute for Frontier Medical Sciences, Kyoto University, Kyoto, Japan
[g] Department of Development and Differentiation, Institute for Frontier Medical Sciences, Kyoto University, Kyoto, Japan
[h] Institute for Integrated Cell-Material Sciences (iCeMS), Kyoto University, Kyoto, Japan

ARTICLE INFO

Article history:
Received 28 December 2008
Revised 10 February 2009
Accepted 21 February 2009
Available online 27 February 2009

Edited by Robert Barouki

Keywords:
Adipogenesis
Adipocyte
Stem cell
Differentiation

ABSTRACT

Induced pluripotent stem (iPS) cells were recently established from human fibroblasts. In the present study we investigated the adipogenic differentiation properties of four human iPS cell lines and compared them with those of two human embryonic stem (ES) cell lines. After 12 days of embryoid body formation and an additional 10 days of differentiation on Poly-L-ornithine and fibronectin-coated dishes with adipogenic differentiation medium, human iPS cells exhibited lipid accumulation and transcription of adipogenesis-related molecules such as C/EBPα, PPARγ2, leptin and aP2. These results demonstrate that human iPS cells have an adipogenic potential comparable to human ES cells.

1. Introduction

Pluripotent embryonic stem (ES) cells have been considered potent candidates for regenerative medicine as an unlimited source of cells for the transplantation therapy and a useful tool for the investigation of cell development/differentiation, especially after establishment of human ES cells [1]. We previously clarified the differentiation process of mouse, monkey and human ES cells into vascular cells [2–4] and demonstrated that transplantation of vascular cells derived from human ES cells may constitute a novel strategy for vascular regeneration [4,5]. A number of immunological and ethical problems remain to be overcome before clinical application of the ES cells, however. Recently, novel ES cell-like pluripotent cells, termed induced pluripotent stem (iPS) cells, were generated by introducing four transcription factors (Oct3/4, Sox2, Klf4 and c-Myc) into mouse skin fibroblasts [6], and soon thereafter iPS cells were also generated from human skin fibroblasts [7,8]. Since then, a new generation of human iPS cells has been generated by introducing into fibroblasts just three of the aforementioned transcription factors (c-Myc was omitted) [9]. By overcoming the immunological and ethical problems associated with ES cells, iPS cells open a new avenue for cell transplantation-based regenerative medicine and provide a powerful new tool with which to investigate organ development/differentiation in specific disease states, especially in inherited diseases.

Generalized lipodystrophy consists of congenital and acquired types characterized by the lack of the whole adipose tissue, which leads to severe insulin-resistant diabetes, hypertriglyceridemia and fatty liver. We previously analyzed genes and phenotypes of congenital generalized lipodystrophic Japanese [10] and also demonstrated the long-lasting efficacy and safety of the leptin-replacement therapy in these patients [11–13]. Since metabolic abnormality in the mouse model is known to be cured by mature

* Corresponding authors. Fax: +81 75 771 9452.
E-mail addresses: sonemasa@kuhp.kyoto-u.ac.jp (M. Sone), kh@kuhp.kyoto-u.ac.jp (K. Hosoda).
[1] These authors contributed equally to this work.

0014-5793/$36.00
doi:10.1016/j.febslet.2009.02.031

adipocytes transplantation, the regeneration therapy of the adipose tissue with human iPS cells-derived adipocytes is the ideal goal for lipodystrophic patients. Moreover, in vitro adipogenic differentiation system of human iPS cells will contribute to elucidate the pathogenesis of congenital generalized lipodystrophy when iPS cell lines are established from patients with lipodystrophy. In the present study we have investigated the adipogenic differentiation of human iPS cells and compared with that of human ES cells.

2. Materials and methods

2.1. Cells and culture

Four human iPS cell lines (201B6, 201B7, 253G1 and 253G4) were investigated. The 201B6 (B6) and 201B7 (B7) lines were generated by introducing four transcription factors (Oct3/4, Sox2, Klf4 and c-Myc) into human skin fibroblasts while the 253G1 (G1) and 253G4 (G4) lines were generated using only three factors (c-Myc was omitted) [9]. These iPS cell lines were maintained as previously described [7]. Two human ES cell lines (H9 and KhES-1) were used and maintained as previously described [1,14].

2.2. Adipogenic differentiation

For embryoid body (EB) formation, iPS and ES colonies were digested with 1 mg/ml collagenase type IV (GIBCO, CA, USA) and plated onto non-adherent bacterial culture dishes, where they were allowed to aggregate in maintenance medium without bFGF. Retinoic acid (Sigma–Aldrich, Japan) was added to the medium to a concentration of 100 nM from day 2 to day 5. After 12 days, EBs were transferred to 6-well plates coated with a combination of 30 μg/ml Poly-L-ornithine (Sigma–Aldrich) and 2 μg/ml fibronectin (Sigma–Aldrich). To induce adipocyte differentiation from iPS and ES cells, we applied a modification of a procedure described previously for use with mouse and human ES cells (Fig. 1) [15–19]. Differentiation was induced for 10 days using medium consisting of DMEM-F12, 10% KSR, and an adipogenic cocktail (0.5 mM IBMX, 0.25 μM dexamethasone, 1 μg/ml insulin, 0.2 mM indomethacin and 1 μM pioglitazone).

2.3. Immunocytochemistry

Immunocytochemistry was carried out as previously described [7]. The anti-human primary antibodies included Nanog (R&D Systems, MN, USA) and Alexa 488-conjugated SSEA-4 (Santa Cruz Biotechnology Inc., CA, USA) and TRA1-60 (CHEMICON, LA, USA). The TRA1-60 antibody was labeled using an Alexa Fluor 488 Monoclonal Antibody Labeling Kit (Molecular Probes, OR, USA). Alexa 546-conjugated donkey anti-sheep IgG (Molecular Probes, OR, USA) served as the secondary antibody. Alkaline phosphatase activity was detected using a BCIP/NBT substrate system (Dakocytomation, CA, USA).

2.4. Oil Red O staining and microscopic analysis of adipocytes

Cells were washed with phosphate-buffered saline (PBS) twice, fixed in 3.7% formaldehyde for 1 h and then stained with 0.6% (w/v) Oil Red O (Nacalai Tesque, Japan) solution (60% isopropanol, 40% water) for 2 h at room temperature. The cells were then washed with water to remove unbound dye. Subsequently, the bound Oil Red O was eluted with isopropanol.

After staining with Oil Red O, each EB was examined microscopically for the presence of adipocyte colonies, and the percentage of EBs with outgrowths showing adipocyte positivity was determined as previously described [15]. EBs in which adipocytes accounted for more than half of their circumference were considered adipocyte-positive. The percent area of Oil Red O staining (+) was determined at 20× magnification by counting the number of pixels exhibiting Oil Red O positivity in selected microscope fields (449 × 338 pixels). Four randomly selected fields were examined in each well of a 6-well plate, and the percent area was calculated as the average for the four fields. Six independent experiments were performed for each cell line.

Table 1
Primers for reverse-transcription polymerase chain reaction.

Gene		Sequence
Nanog	Sense	CAGCCCCGATTCTTCCACCAGTCCC
	Antisense	CGGAAGATTCCCAGTCGGGTTCACC
PPARγ2	Sense	ATTGACCCAGAAAGCGATTC
	Antisense	CAAAGGAGTGGGAGTGGTCT
C/EBPα	Sense	GCAAACTCACCGCTCCAATG
	Antisense	TTAGGTTCCAAGCCCCAAGTC
aP2	Sense	AACCTTAGATGGGGGTGTCCTG
	Antisense	TCGTGGAAGTGACGCCTTTC
Leptin	Sense	GAACCCTGTGCGGATTCTTGTG
	Antisense	CGTTTCTTFAAGGCATACTGGTGAG
GAPDH	Sense	ACCACAGTCCATGCCATCAC
	Antisense	TCCACCACCCTGTTGCTGT
PPARγ2 (real-time RT-PCR)	Sense	GATACACTGTCTGCAAACATATCACAA
	Antisense	CCACGGAGCTGATCCCAA
	Probe	AGAGATGCCATTCTGGCCCACCAACTT

2.5. Reverse-transcription polymerase chain reaction (RT-PCR) and quantitative real-time PCR

Total RNA was extracted using TRizol Reagent (Invitrogen, CA, USA) and treated with RNase-Free DNase Set (QIAGEN, Germany) to remove any contaminating genomic DNA. For RT-PCR, cDNA was synthesized using a PrimeScript RT reagent Kit (Takara Bio Inc., Japan), after which RT-PCR was run using ExTaq (Takara Bio Inc.). For quantitative real-time PCR, TaqMan PCR was carried out using a Step One Plus Real-Time PCR System as instructed by the manufacturer (Applied Biosystems, CA, USA). Levels of mRNA were normalized to those of 18S mRNA. The primers used are listed in Table 1.

2.6. Statistical analysis

Data are expressed as means ± S.E.M. Statistical significance was evaluated using ANOVA for comparison among six groups. Values of $P < 0.05$ were considered significant.

3. Results

3.1. Adipogenic differentiation of human iPS and ES cells

Morphological phenotypes, immunoreactivities of Nanog, SSEA-4 and TRA-1-60, and ALP activity of human iPS cells did not differ

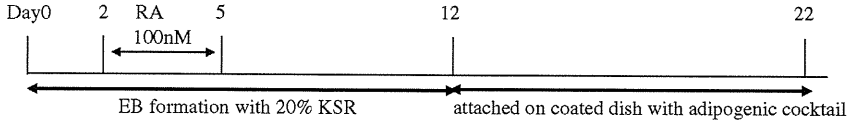

Fig. 1. Schematic diagram of the experimental protocol used for adipocyte differentiation from human ES and human iPS cells. EB: embryoid body. Adipogenic cocktail: 0.5 mM IBMX, 0.25 μM dexamethasone, 1 μg/ml insulin, 0.2 mM indomethacin and 1 μM pioglitazone.

from those of human ES cells (Fig. 2). In order to assess their potential for adipogenic differentiation, the human iPS cells were subjected to adipogenic induction culture. After 12 days of EB formation, EBs derived from human iPS cells were attached to coated dishes to induce differentiation. Several kinds of coating for the dishes, including gelatin, collagen IV and fibronectin were compared, and the efficiency of EB attachment and adipogenic differentiation were the best on dishes coated with a combination of Poly-L-ornithine and fibronectin. On day 15, after 3 days of adipogenic differentiation following the EB formation, differentiated cells containing small cytoplasmic lipid droplets were observed spreading outward from the attached EBs. On day 22, the lipid accumulation was evaluated by staining the cells with Oil Red O.

To evaluate the adipogenic potential of individual iPS cell lines, the percentage of EB outgrowths having adipocyte colonies and the percent area of Oil Red O staining (+) were determined. For each of iPS and ES cell lines tested, 40–60% of EBs formed adipocyte colonies (Table 2). In all of the iPS cell lines, lipid accumulation was similar to that seen in human ES cell lines (Fig. 3), though the B7 line showed stronger lipid accumulation than the other cell lines.

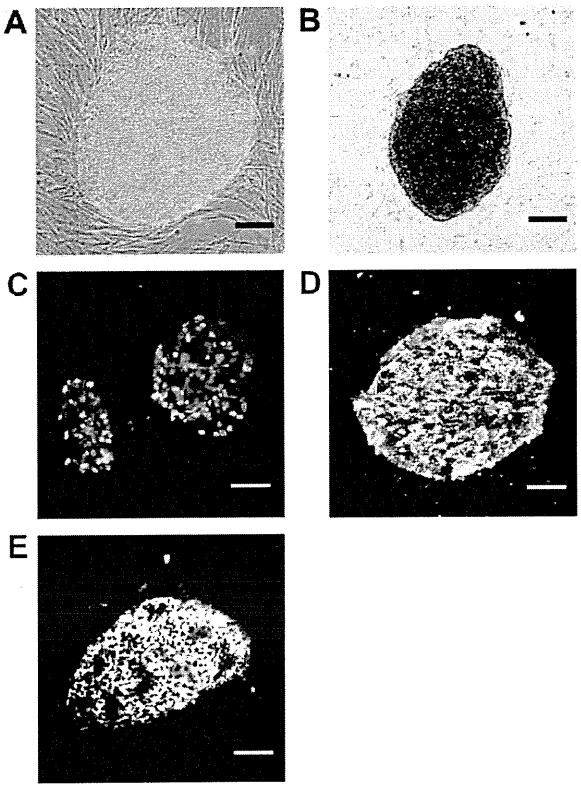

Fig. 2. Morphology of undifferentiated human iPS cells (G4). (A) Phase-contrast photomicrograph of an undifferentiated colony. (B) Alkaline phosphatase activity. (C) Immunofluorescent staining with Nanog. (D) Immunofluorescent staining with SSEA-4. (E) Immunofluorescent staining with TRA1-60. Scale bar = 100 μM.

Table 2
% of EBs with adipocyte colonies.

Cell line	[Number of EBs with adipocytecolonies/total number of EBs]
201B6	54.1% [40/74]
201B7	59.7% [46/77]
253G1	50.0% [35/70]
253G4	56.4% [44/78]
H9	48.8% [39/80]
KhES-1	45.5% [35/77]

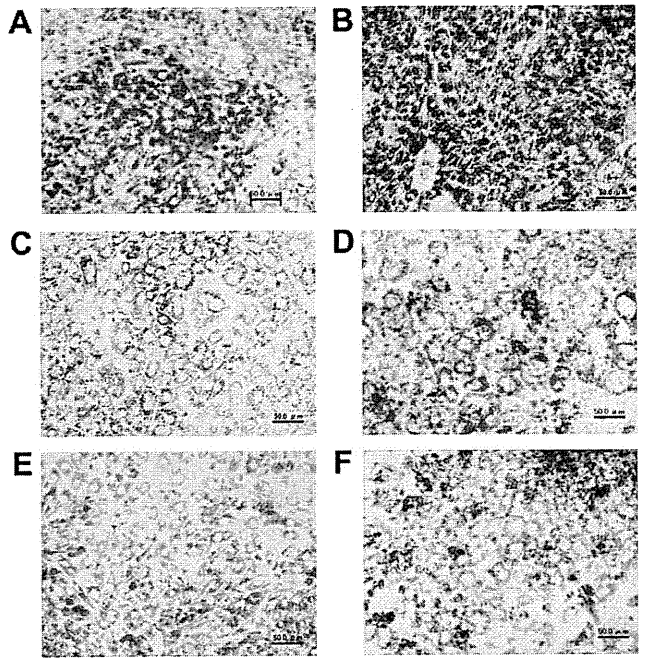

Fig. 3. Oil Red O staining of adipocytes derived from human iPS cells (A–D) and ES cells (E, F) on day 22. B6 (B) B7 (C) G1 (D) G4 (E) H9 (F) KhES-1. Scale bar = 50 μM.

Statistical analysis of the percent area of Oil Red O staining (+) showed no significant differences among the cell lines (Fig. 4).

3.2. Expression of adipogenesis-related molecules

Using RT-PCR, transcription of adipogenic markers was investigated on days 0 and 22 of differentiation (Fig. 5A). Though not detected at day 0, mRNAs encoding the adipogenic transcription factors C/EBPα (CCAAT/enhancer binding protein α) and PPARγ2 (peroxisome proliferator-activated receptor γ2) were detected on day 22. In contrast, expression of Nanog mRNA was strongly suppressed on day 22, as compared with its expression on day 0. Expression of the mature adipocyte markers leptin and aP2 (adipocyte fatty acid binding protein) was also clearly detected on day 22. All of the human iPS cell lines expressed mRNAs encoding adipogenesis-related molecules at levels that were comparable to the levels seen in human ES cell lines (Fig. 5A). In Quantitative real-time PCR analysis, expression of PPARγ2 mRNA differed somewhat among the iPS and ES cell lines. The differences between the B7 line and the two ES cell lines were significant, but other differences were not significant (Fig. 5B).

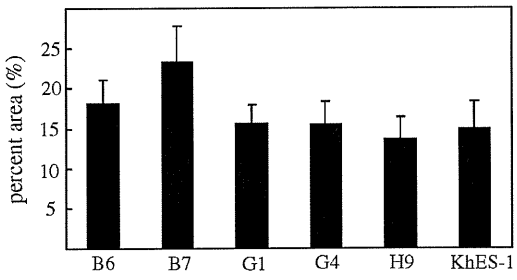

Fig. 4. Percent area of Oil Red O staining. Results are means of six independent experiments. No significant differences were observed among the iPS and ES cell lines.

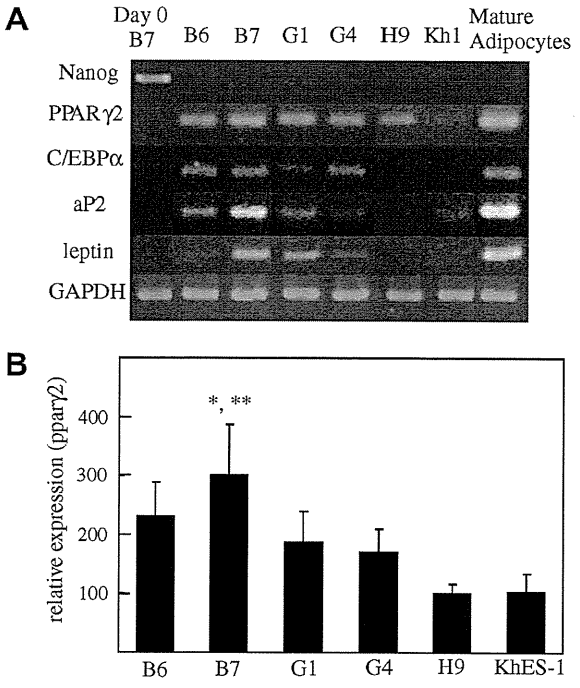

Fig. 5. (A) Transcription of the adipocyte-specific markers PPARγ2, CEBP/α, aP2 and leptin. RNA samples from undifferentiated human iPS cells (B7, day 0) and differentiated stage iPS cells (B6, B7, G1, G4) and human ES cells (H9, KhES-1), as well as mature human adipocytes differentiated from human adipose-derived mesenchymal stem cells (positive control), were analyzed by RT-PCR. Nanog is an undifferentiated human ES cell marker. GAPDH served as an internal standard for RT-PCR. Kh1: KhES-1. Adipose: human mature adipocytes differentiated from human adipose-derived mesenchymal stem cells. (B) Relative levels of PPARγ2 mRNA expression are shown as means ± S.E.M. of 4–6 independent experiments and normalized to those of 18S. The levels are expressed as percentages of the expression in the H9 cell line. $^{*}P < 0.05$ vs. H9. $^{**}P < 0.05$ vs. KhES-1.

4. Discussion

The present study demonstrates that human iPS cells have adipogenic potential comparable to human ES cells. Four human iPS cell lines of two generations were investigated. The B6 and B7 were generated by introducing four transcription factors (Oct3/4, Sox2, Klf4 and c-Myc) into human skin fibroblasts while the G1 and G4 were generated using only three factors (c-Myc was omitted) [9]. After 12 days of embryoid body formation and an additional 10 days of differentiation on Poly-L-ornithine and fibronectin-coated dishes with adipogenic differentiation medium, all human iPS cell lines of both generations exhibited lipid accumulation and transcription of such adipogenesis-related molecules as C/EBPα, PPARγ2, leptin and aP2. We also compared differentiation efficiency between human iPS and ES cells using two lines of human ES cells and found no apparent difference between human iPS and ES cells in properties of adipogenic differentiation including the time course and potential. In terms of lipid accumulation and transcription of adipogenesis-related molecules, human iPS-derived adipocytes appear to reach at least the same level of maturity as those derived from human ES cells. The B7 line tended to show stronger adipogenic potential than the other five iPS lines and the ES cell lines, but the difference in terms of percent area of Oil Red O staining (+) was not significant. The B7 line also showed significantly stronger expression of PPARγ2 than the two ES cell lines tested, but PPARγ2 expression varied among the different iPS cell lines, despite their having the same genetic background. We conclude that the adipogenic potential of iPS cells did not essentially differ from ES cells, though their adipogenic potentials were rather varied in each line.

Despite the prevalence of obesity, systems for research into human adipocyte biology remain underdeveloped, in part because of a lack of available human adipocyte cell lines. There are significant differences between adipocyte development in humans and mice [20]. The established in vitro adipocyte differentiation system using human iPS cells in the present study should make it possible to dissect out the cellular mechanisms underlying human adipocyte differentiation. It should also contribute to the better understanding of adipocyte biology and serve as a basis for advances in research into obesity and adipotoxicity, which has been proposed as the sum of the negative effects associated with obesity [21].

Adipogenesis is largely divided into two phases: the early phase consisting of the lineage commitment of adipocytes from pluripotent stem cells and the late phase consisting of the terminal differentiation of preadipocytes into adipocytes [22]. The molecular mechanism underlying the terminal adipocyte differentiation has been identified through analysis of the differentiation process in immortalized mouse preadipocyte cell lines (e.g., 3T3-L1 and 3T3-F442A cells) [22–24], but the differentiation from pluripotent stem cells during the early stage of adipogenesis must await further clarification. The establishment of adipocyte differentiation system with human iPS cells should facilitate that line of research.

In contrast to human ES cells, iPS cells can be induced from any human being irrespective of their genetic make-up. Consequently, the study of iPS cells should contribute to the identification of new susceptibility genes associated with obesity and metabolic syndrome, and to the clarification of the functions of those genes. The establishment of iPS cell lines from patients with inherited diseases presenting adipocyte abnormality should enable clarification of their pathogenesis. And because they overcome the immunological and ethical problems associated with human ES cells, iPS cell systems should also contribute to the development of novel regenerative therapies for reconstruction of soft tissue defects after tumor resections, extensive deep burns and lipodystrophy. The induced cells obtained with our protocol are not a homogeneous population. Consequently, at this stage human iPS cells may not yet have as much adipogenic potential as adipose-derived stem cells (ADSCs), which are derived from the stromal vascular fraction of human adipose tissue and are thought to be a safe and useful tool in adipose regenerative medicine [25]. About 80% of ADSCs differentiate into adipocytes under suitable conditions [26]. The next issue we plan to address will be the establishment of an improved differentiation protocol that includes a purification process such as cell sorting.

In conclusion, the present study demonstrates that human iPS cells have adipogenic potential that is generally equal to that of human ES cells. The use of iPS cells will contribute to the development of regenerative therapies of adipose tissue for lipodystrophy. This work should also contribute to our understanding of human adipogenesis and to the clarification of the pathogenesis and pathophysiology of obesity and metabolic syndrome, potentially leading to the development of new drug therapies.

Acknowledgement

We thank Yoshie Fukuchi for her technical assistance. This work was supported by the project for realization of regenerative medicine of the Ministry of Education, Culture, Sports, Science and Technology, Japan.

References

[1] Thomson, J.A., Itskovitz-Eldor, J., Shapiro, S.S., Waknitz, M.A., Swiergiel, J.J., Marshall, V.S. and Jones, J.M. (1998) Embryonic stem cell lines derived from human blastocytsts. Science 282, 1145–1147.

[2] Yamashita, J., Itoh, H., Hirashima, M., Ogawa, M., Nishikawa, S., Yurugi, T., Naito, M., Nakao, K., Nishikawa, S., et al. (2000) Flk1-positive cells derived from embryonic stem cells serve as vascular progenitors. Nature 408, 92–96.
[3] Sone, M., Itoh, H., Yamashita, J., Nakao, K., et al. (2003) Different differentiation kinetics of vascular progenitor cells in primate and mouse embryonic stem cells. Circulation 107, 2085–2088.
[4] Sone, M., Itoh, H., Nakao, K., et al. (2007) Pathway for differentiation of human embryonic stem cells to vascular cell components and their potential for vascular regeneration. Arterioscler. Thromb. Vasc. Biol. 27, 2127–2134.
[5] Yamahara, K., Sone, M., Itoh, H., Nakao, K., et al. (2008) Augmentation of Neovascularizaition in hindlimb ischemia by combined transplantation of human embryonic stem cells-derived endothelial and mural cells. PLOS One 3 (2), e1666.
[6] Takahashi, K. and Yamanaka, S. (2006) Induction of pluripotent stem cells from mouse embryonic and adult fibroblast cultures by defined factors. Cell 126, 663–676.
[7] Takahashi, K., Tanabe, K., Ohnuki, M., Narita, M., Ichisaka, T., Tomoda, K. and Yamanaka, S. (2007) Induction of pluripotent stem cells from adult human fibroblasts by defined factors. Cell 131, 861–872.
[8] Yu, J., Vodyanik, M.A., Smuga-Otto, K., Antosiewicz-Bourget, J., Frane, J.L., Tian, S., Nie, J., Jonsdottir, G.A., Ruotti, V., Stewart, R., Slukvin II and Thomson, J.A. (2007) Induced pluripotent stem cell lines derived from human somatic cells. Science 318, 1917–1920.
[9] Nakagawa, M., Koyanagi, M., Tanabe, K., Takahashi, K., Ichisaka, T., Aoi, T., Okita, K., Mochiduki, Y., Takizawa, N. and Yamanaka, S. (2008) Generation of induced pluripotent stem cells without Myc from mouse and human fibroblasts. Nat. Biotechnol. 26, 101–106.
[10] Ebihara, K., Kusakabe, T., Masuzaki, H., Kobayashi, N., Tanaka, T., Chusho, H., Miyanaga, F., Miyazawa, T., Hayashi, T., Hosoda, K., Ogawa, Y. and Nakao, K. (2004) Gene and phenotype analysis of congenital generalized lipodystrophy in Japanese: a novel homozygous nonsense mutation in seipin gene. J. Clin. Endocrinol. Metab. 89 (5), 2360–2364.
[11] Ebihara, K., Masuzaki, H. and Nakao, K. (2004) Long-term leptin-replacement therapy for lipoatrophic diabetes. New Engl. J. Med. 351 (6), 615–616.
[12] Ebihara, K., Kusakabe, T., Hirata, M., Masuzaki, H., Miyanaga, F., Kobayashi, N., Tanaka, T., Chusho, H., Miyazawa, T., Hayashi, T., Hosoda, K., Ogawa, Y., DePaoli, AM., Fukushima, M. and Nakao, K. (2007) Efficacy and safety of leptin-replacement therapy and possible mechanisms of leptin actions in patients with generalized lipodystrophy. J. Clin. Endocrinol. Metab. 92 (2), 532–541.
[13] Ebihara, K., Ogawa, Y., Masuzaki, H., Shintani, M., Miyanaga, F., Aizawa-Abe, M., Hayashi, T., Hosoda, K., Inoue, G., Yoshimasa, Y., Gavrilova, O., Reitman, ML. and Nakao, K. (2001) Transgenic overexpression of leptin rescues insulin resistance and diabetes in a mouse model of lipoatrophic diabetes. Diabetes 50 (6), 1440–1448.
[14] Fujioka, T., Yasuchika, K., Nakamura, Y., Nakatsuji, N. and Suemori, H. (2004) A simple and efficient cryopreservation method for primate embryonic stem cells. Int. J. Dev. Biol. 48, 1149–1154.
[15] Dani, C., Smith, A.G., Ailhaud, G., et al. (1997) Differentiation of embryonic stem cells into adipocytes in vitro. J. Cell. Sci. 110, 1279–1285.
[16] Xiong, C., Xie, C.Q., Chen, Y.E., et al. (2005) Derivation of adipocytes from human embryonic stem cells. Stem Cells Dev. 14, 671–675.
[17] van Harmelen, V., Astrom, G., Ryden, M., et al. (2007) Differential lipolytic regulation in human embryonic stem cell-derived adipocytes. Obesity 15, 846–852.
[18] Barberi, T., Willis, L.M., Socci, N.D. and Studer, L. (2005) Derivation of multipotent mesenchymal precursors from human embryonic stem cells. PLoS Med. 2, e161.
[19] Olivier, E.N., Rybicki, A.C. and Bouhassira, E.E. (2006) Differentiation of human embryonic stem cells into bipotent mesenchymal stem cells. Stem cells 24, 1914–1922.
[20] Arner, P. (2005) Resistin: yet another adipokine tells us that men are not mice. Diabetologia 48, 2203–2205.
[21] Nakao, K. (2009) Adiposcience and adipotoxicity. Nat. Clin. Pract. Endocrinol. Metab. 5 (2), 63.
[22] Rosen, E.D. and Spiegelman, B.M. (2000) Molecular regulation of adipogenesis. Annu. Rev. Cell. Dev. Biol. 16, 145–171.
[23] Bernlohr, D.A., Bolanowski, M.A., Kelly Jr., T.J. and Lane, M.D. (1985) Evidence for an increase in transcription of specific mRNAs during differentiation of 3T3-L1 preadipocytes. J. Biol. Chem. 260, 5563–5567.
[24] Flier, J.S. (2004) Obesity wars: molecular progress confronts an expanding epidemic. Cell 116, 337–350.
[25] Zuk, P.A., Zhu, M., Mizuno, H., Huang, J., Futrell, J.W., et al. (2001) Multilineage cells from human adipose tissue: Implications for cell-based therapies. Tissue Eng. 7, 211–228.
[26] Zhu, Y., Liu, T., Song, K., Fan, X., Ma, X. and Cui, Z. (2008) Adipose-derived stem cell: a better stem cell than BMSC. Cell Biochem. Funct. 26, 664–675.

Induction and Isolation of Vascular Cells From Human Induced Pluripotent Stem Cells—Brief Report

Daisuke Taura, Masakatsu Sone, Koichiro Homma, Naofumi Oyamada, Kazutoshi Takahashi, Naohisa Tamura, Shinya Yamanaka, Kazuwa Nakao

Objective—Induced pluripotent stem (iPS) cells are a novel stem cell population derived from human adult somatic cells through reprogramming using a defined set of transcription factors. Our aim was to determine the features of the directed differentiation of human iPS cells into vascular endothelial cells (ECs) and mural cells (MCs), and to compare that process with human embryonic stem (hES) cells.

Methods and Results—We previously established a system for differentiating hES cells into vascular cells. We applied this system to human iPS cells and examined their directed differentiation. After differentiation, TRA1–60$^-$ Flk1$^+$ cells emerged and divided into VE-cadherin–positive and –negative populations. The former were also positive for CD34, CD31, and eNOS and were consistent with ECs. The latter differentiated into MCs, which expressed smooth muscle α-actin and calponin after further differentiation. The efficiency of the differentiation was comparable to that of human ES cells.

Conclusions—We succeeded in inducing and isolating human vascular cells from iPS cells and indicate that the properties of human iPS cell differentiation into vascular cells are nearly identical to those of hES cells. This work will contribute to our understanding of human vascular differentiation/development and to the development of vascular regenerative medicine. (***Arterioscler Thromb Vasc Biol.* 2009;29:1100-1103.)**

Key Words: angiogenesis ■ stem cells ■ vascular biology ■ endothelium ■ differentiation

Pluripotent embryonic stem (ES) cells are thought to represent a potentially unlimited pool from which to derive cells for new treatments in the area of regenerative medicine and for investigation of cell development/differentiation. We previously described the process by which mouse, monkey and human embryonic stem (ES) cells differentiate into vascular cells.[1,2,3] In addition, we used the hindlimb ischemia model with immunodeficient mice to demonstrate that transplanted vascular endothelial cells (ECs) and mural cells (MCs) derived from human (h)ES cells could be successfully incorporated into the host vasculature and significantly accelerate improvements in local blood flow.[3,4] However, immunologic and ethical problems remain to be overcome before clinical application.

Recently, novel ES cell-like pluripotent cells were generated from mouse skin fibroblasts by introducing 4 transcription factors.[5] Termed induced pluripotent stem (iPS) cells, they were subsequently generated from human skin fibroblasts.[6,7] At present, the properties of human iPS cell differentiation into vascular cells remain unknown. To address that issue, we investigated the differentiation of human iPS cells into ECs and MCs using our differentiation system previously developed for hES cells.

Materials and Methods

Cell Culture

hES, human iPS, and OP9 feeder cells were all established and maintained as described previously.[6,8,9] To induce differentiation, hES or iPS cells were cultured on an OP9 feeder layer as described previously.[3]

Flow Cytometry and Cell Sorting

Flow cytometric analysis and cell sorting were performed as described previously.[1,9]

Immunohistochemistry

Cultured cells were stained with various monoclonal antibodies as described.[1,9]

For details regarding cell culture, RT-PCR, and the antibodies used in flow cytometry and immunohistochemistry, please see the supplemental material (available online at http://atvb.ahajournals.org).

Received December 4, 2008; revision accepted April 16, 2009.

From the Department of Medicine and Clinical Science (D.T., M.S., K.H., N.O., N.T., K.N.), Kyoto University Graduate School of Medicine; the Department of Stem Cell Biology (K.T., S.Y.), Institute for Frontier Medical Sciences, Kyoto University; and the Center for iPS Cell Research and Application (CiRA) (K.T., S.Y.), Institute for Integrated Cell-Material Sciences, Kyoto University, Japan.

Correspondence to Masakatsu Sone, MD, PhD, 54 Shogoin Kawahara-cho, Sakyo-ku, Kyoto 606-8507, Japan. E-mail sonemasa@kuhp.kyoto-u.ac.jp

Arterioscler Thromb Vasc Biol is available at http://atvb.ahajournals.org DOI: 10.1161/ATVBAHA.108.182162